Modulation of Gene Expression in Human Central Nervous System Tumors under Methionine Deprivation-induced Stress

Demetrius M. Kokkinakis,[1,2] Xiaoyan Liu,[1] Sunil Chada,[4] Mansoor M. Ahmed,[3] Mohammed M. Shareef,[3] Ujjal K. Singha,[1] Sutin Yang,[1] and Jianhua Luo[2]

[1]The University of Pittsburgh Cancer Institute and the [2]Department of Pathology, Hillman Cancer Institute, Pittsburgh, Pennsylvania; [3]The University of Kentucky Department of Radiation Medicine, Lexington, Kentucky; and [4]Introgen Therapeutics Inc., Houston, Texas

ABSTRACT

Methionine deprivation imposes a metabolic stress, termed methionine stress, that inhibits mitosis and induces cell cycle arrest and apoptosis. The methionine-dependent central nervous system tumor cell lines DAOY (medulloblastoma), SWB61 (anaplastic oligodendroglioma), SWB40 (anaplastic astrocytoma), and SWB39 (glioblastoma multiforme) were compared with methionine-stress resistant SWB77 (glioblastoma multiforme). The cDNA-oligoarray analysis and reverse transcription-PCR verification indicated common changes in gene expression in methionine-dependent cell lines to include up-regulation/induction of cyclin D1, mitotic arrest deficient (MAD)1, p21, growth arrest and DNA-damage-inducible (GADD)45 α, GADD45 γ, GADD34, breast cancer (BRCA)1, 14-3-3σ, B-cell CLL/lymphoma (BCL)1, transforming growth factor (TGF)-β, TGF-β–induced early response (TIEG), SMAD5, SMAD7, SMAD2, insulin-like growth factor binding protein (IGFBP7), IGF-R2, vascular endothelial growth factor (VEGF), TNF-related apoptosis-inducing ligand (TRAIL), TNF-α converting enzyme (TACE), TRAIL receptor (TRAIL-R)2, TNFR-related death receptor (DR)6, TRAF interacting protein (I-TRAF), IL-6, MDA7, IL-1B convertase (ICE)-γ, δ and ε, IRF1, IRF5, IRF7, interferon (IFN)-γ and receptor components, ISG15, p65-NF-κB, JUN-B, positive cofactor (PC)4, C/ERB-β, inositol triphosphate receptor I, and methionine adenosyltransferase II. On the other hand, cyclins A1, A2, B1 and B2, cell division cycle (CDC)2 and its kinase, CDC25 A and B, budding uninhibited by benzimidazoles (BUB)1 and 3, MAD2, CDC28 protein kinase (CKS)1 and 2, neuroepithelial cell transforming gene (NET)1, activator of S-phase kinase (ASK), CDC14B phosphatase, BCL2, TGF-β activated kinase (TAK)1, TAB1, c-FOS, DNA topoisomerase II, DNA polymerase α, dihydrofolate reductase, thymidine kinase, stathmin, and MAP4 were down-regulated. In the methionine stress-resistant SWB77, only 20% of the above genes were affected, and then only to a lesser extent. In addition, some of the changes observed in SWB77 were opposite to those seen in methionine-dependent tumors, including expression of p21, TRAIL-R2, and TIEG. Despite similarities, differences between methionine-dependent tumors were substantial, especially in regard to regulation of cytokine expression. Western blot analysis confirmed that methionine stress caused the following: (a) a marked increase of GADD45α and γ in the wt-p53 cell lines SWB61 and 40; (b) an increase in GADD34 and p21 protein in all of the methionine-dependent lines; and (c) the induction of MDA7 and phospho-p38 in DAOY and SWB39, consistent with marked transcriptional activation of the former under methionine stress. It was additionally shown that methionine stress down-regulated the highly active phosphatidylinositol 3′-kinase pathway by reducing AKT phosphorylation, especially in DAOY and SWB77, and also reduced the levels of retinoblastoma (Rb) and pRb (P-ser780, P-ser795, and P-ser807/811), resulting in a shift in favor of unphosphorylated species in all of the methionine-dependent lines. Immunohistochemical analysis showed marked inhibition of nuclear translocation of nuclear factor κB under methionine stress in methionine-dependent lines. In this study we show for the first time that methionine stress mobilizes several defined cell cycle checkpoints and proapoptotic pathways while coordinately inhibiting prosurvival mechanisms in central nervous system tumors. It is clear that methionine stress-induced cytotoxicity is not restricted by the p53 mutational status.

INTRODUCTION

Most human tumor cells are dependent on exogenous methionine, whereas normal tissues can rely on homocysteine to meet their methionine needs (1). This is known as the methionine defect, and although it has been attributed to failure of methionine synthase to recycle homocysteine in rapidly dividing cells (2), its cause is far more complex and may involve altered methylation patterns in tumor DNA that affect gene expression. Because of the property of methionine stress to target only cancer and not normal cells, its potential for clinical use against many malignancies has outweighed the technical problems encountered in the past (3, 4) that have kept this approach in obscurity. Theoretically, methionine-dependent tumors could be selectively "starved" under methionine-stress conditions, whereas normal tissues are rescued with homocysteine. This theory was validated in central nervous system (CNS) tumor xenografts implanted in athymic mice with both dietary and pharmacological suppression of methionine (3, 4). Methionine-depleting regimens caused three distinct physiologic responses: (a) mitotic and cell cycle blocks, which lead to cell death and a marked and sustained regression during methionine-depleting regimens (5); (b) selective sensitization of tumors to DNA alkylating damaging agents because of down-regulation of DNA repair protein O^6-methylguanine-DNA methyltransferase (3–6); and (c) a marked increase in the immune response of the host against tumors indicated by the macrophage infiltration (4).

Given the similar response of CNS tumors to methionine stress, it is possible that the restriction of methionine mobilizes cellular elements for growth control and death that are common in these tumors. The effect of methionine stress may be exerted via the induction of a single gene with multiple regulatory functions leading to proapoptotic and/or antisurvival events such as p53. The alternative to a single gene involvement is the mobilization of several proapoptotic or antiproliferative elements acting via a variety of mechanisms that are either common or depend on the mutational status of the tumor cell. A marked up-regulation of more than a single tumor suppressor gene or of a single signal transduction pathway by methionine stress could result in a synergy that would be more toxic to tumors than the targeting of a single gene or gene product. Whether the toxicity of methionine stress is regulated by the induction of a single or by multiple tumor suppressor genes, such toxicity should also depend on how the methionine stress influences the induction of proapoptotic and/or the abrogation of prosurvival (proliferative) pathways by altering signal transduction patterns through direct regulation of growth factors and epigenetic events. Because of the complexity of testing this hypothesis, understanding methionine stress requires the use of holistic approaches to identify the multiple changes in gene expression and protein synthesis between this stress and the normal condi-

tion. To determine the effect of methionine stress on gene expression in CNS tumors, and to subsequently link key elements of gene expression to physiologic effects of the stress, such as cell cycle arrest and apoptosis, we compared gene expression and key protein synthesis profiles between pairs of CNS tumor cells cultured either in methionine or homocysteine in the following set of lines: (*a*) the glioblastoma multiforme SWB77 (mut p53), which is resistant to methionine stress in xenograft experiments (4); (*b*) the glioblastoma multiforme SWB39 (mut p53); (*c*) the meduloblastoma DAOY (mut p53), which is sensitive to methionine stress both in culture and in xenograft experiments (3–5); (*d*) the anaplastic oligodendroglioma SWB61 (wt p53); and (*e*) the anaplastic astrocytoma SWB40 (wt p53). In this article we show that methionine stress in CNS tumors induces cell cycle inhibition and proapoptotic events regardless of p53 mutational status and inhibits prosurvival pathways by partially overlapping mechanisms.

MATERIALS AND METHODS

Cell Lines and Culture. The CNS tumor cell lines SWB40 (anaplastic astrocytoma), SWB61 (anaplastic oligodendroglioma), SWB77 (glioblastoma multiforme), and SWB39 (glioblastoma multiforme), which have been isolated and characterized in this laboratory (7), as well as the medulloblastoma DAOY and the modified fibroblast 3T3 (American Type Culture Collection, Manassas, VA) were used in this study. Additional cell lines, namely SWB85, SWB83, SWB95, and SWB33, also isolated in this laboratory from glioblastoma multiformes were used in some experiments. All of the cell lines were cultured in DMEM (BioWhittaker, Walkersville, MD) with 5% fetal bovine serum (Media Tech, Inc., Herndon, VA) in 6.5% CO_2 atmosphere at 37°C until confluent. Cultures were subsequently adapted to DMEM A (Media Tech, Inc.) supplemented with an additional 584 mg/L L-glutamine (Sigma, St. Louis, MO) to a final concentration of 8 mmol/L, 10 ml/L of Pen/Strep (Sigma), and 50 ml/L dialyzed fetal bovine serum (Life Technologies, Inc., Grand Island, NY). Once the cell lines were passed three times in medium A, they were split into 40 T-75 flasks and maintained in medium A until they reached 60 to 70% confluence. At that time, 10 plates were maintained in medium A, whereas the rest were transferred in methionine-free DMEM B (Media Tech, Inc.) supplemented with 27 mg/L homocysteine thiolactone hydrochloride (Sigma), 62.5 mg/L L-cystine dihydrochloride (Sigma), and L-glutamine to a final concentration of 8 mmol/L, Pen/Strep, and dialyzed fetal bovine serum. Media was replaced in all of the cultures every 48 hours, and detached cells were collected, counted, and processed for determining apoptosis by the terminal deoxynucleotidyl transferase-mediated nick end labeling assay. Growth patterns were observed on a daily basis, and plates were sacrificed approximately every two days to determine cell number progression in each culture and cell cycle measurement by flow cytometry. Additional plates were used to harvest cells at various intervals as indicated one day after medium replacement and frozen at −80°C until used for c-DNA oligoarray and protein analysis.

Flow Cytometry. Cells were trypsinized, washed with PBS twice, and centrifuged (300 rpm) at 4°C. The cell count was adjusted to 2 to 3×10^5/ml cells in PBS per sample. From this cell suspension, 1 ml was taken in duplicate centrifuged at 300 rpm for 10 minutes at 4°C, reduced to 100 μL, and fixed in 500 μL of ice-cold 70% ethanol overnight at 4°C. Fixed cells were centrifuged at 500 rpm at 4°C for 10 minutes and suspended in 500 μL of PBS containing 50 μL of 50 μg/ml propidium iodide (Sigma) and 10 μL of 5 μg/ml RNase for 45 to 60 minutes at 4°C. Flow cytometric analysis was done within 3 hours of propidium iodide staining on a Beckman-Coulter Epics XL. EXPO32 software was used for optimum analysis of cell cycle (G_1, G_2, and S phase).

RNA Isolation and Processing. Total RNA was isolated from control and methionine-stressed lines (at 24 hours before massive apoptosis) in triplicate with a two-step isolation procedure as follows: (1) RNA from the cell samples was extracted with TRIzol reagent; and (2) small fragments of RNA and genomic DNA contamination were eliminated by additionally purifying the total RNA with RNEASY columns. The quality of the RNA samples was examined by quantifying the 260:280 ratio (the minimal acceptable ratio is 1.8) and by visualizing the 28S to 18S rRNA bands in agarose gel (the minimal

acceptable ratio is 1.5). The first-strand cDNA synthesis was carried out with 5 μg total RNA with a T7-d(T)24 primer GGCCAGTGAATTGTAATAC-GACTCACTATAGGGAGGCGG-(dT)24 (Superscript II, Life Technologies, Inc., Rockville, MD). This was followed by the second-strand cDNA synthesis at 16°C by adding *Escherichia coli* (*E. coli*) DNA ligase, *E. coli* DNA polymerase I, and RNase H into the reaction. The cDNA was blunt-ended by the addition of T4 DNA polymerase and purified with phenol/chloroform extractions and ethanol precipitation. The cDNA was then incubated at 37°C for 4 hours in an *in vitro* transcription reaction to produce biotin-labeled cRNA with the MEGAscript system (Ambion, Inc., Austin, TX).

Affymetrix Chip Hybridization. The mRNA expression of over 22,000 genes and expression sequence tags was done for pairs of tumor cells grown in methionine or homocysteine media with the use of U133A (22,000 genes) and U95 (12,600 genes) chips from Affymetrix in duplicate. Briefly, 15 to 20 μg of biotin-labeled cRNA was fragmented by incubating in a buffer containing 200 mmol/L Tris acetate (pH8.1), 500 mmol/L KOAc, and 150 mmol/L MgOAc at 95°C for 35 minutes. The fragmented cDNA was hybridized with a pre-equilibrated Affymetrix chip at 45°C for 14 to 16 hours. The hybridizations were washed in a fluidic station with nonstringent buffer (6 × SSPE, 0.01% Tween 20, and 0.005% antifoam) for 10 cycles and stringent buffer (100 mmol/L 2N-morpholino-ethanesulfonic acid, 0.1 M NaCl, and 0.01% Tween 20) for 4 cycles and stained with strepto-avidin phycoerythrin. This was followed by incubation with biotinylated mouse antiavidin antibody and restained with strepto-avidin phycoerythrin. The chips were scanned in an Agilent ChipScanner (Affymetrix Inc., Santa Clara, CA) to detect hybridization signals. Baseline analyses were done with Oligoarray suite 5.0 to identify statistically significant gene expression alterations between samples derived from cells grown in methionine and those maintained in homocysteine containing medium. Because samples were analyzed in triplicates, these results were additionally screened for consistent *P* by the student *t* tests ($P < 0.05$) to eliminate random sampling errors.

Validation of Affymetrix Chip Hybridization by Real-Time Quantitative PCR. Cyber green light cycler PCR was used to estimate relative mRNA expression with high confidence. An aliquot (200 ng total RNA) of the first-strand cDNA was added to a mastermix of forward and reverse primer mix (30 pmol), SYBR green, two OmniMix HS beads (TaKaRa Bio Inc., Otsu, Shiga, Japan) containing 3 units TaKaRa hot start Taq polymerase, 200 μmol/L deoxynucleoside triphosphate, and 4 mmol/L $MgCl_2$ in 25 mmol/L HEPES buffer (pH 8.0). PCR was done with the following custom primers: inhibitory κB (IκB)e, 5′-GCT GGA AGC ACT CAC TTA CAT CT-3′ (forward) and 5′-GGA GTG CTG TCT GGT AAA GGT TAT-3′ (reverse); NF-κB65, 5′-AGG ACA TAT GAG ACC TTC AAG AGC-3′ and 5′-CTC ATC ATA GTT GAT GGT GCT CAG-3′; RkB, 5′-CTT AAG GGA AGT GAA AGA GGA GTG-3′ and 5′-CAC TGT CCC CCA GTT CTA CTT TAT-3′; NF-κB, 5′-TGG ACA GTA CTA CCT ACG ATG GAA-3′ and 5′-AGA GTC ATC CAG GTC ATA GAG AGG-3′; NF-κB p50, 5′-AGA TCT GTA ACT ACG AGG GAC CAG-3′ and 5′-TAG TCC CCA TCA TGT TCT CCT TAG-3′; BAX, 5′-GAC CCA GAG ATG GTC ACC TTA C-3′ and 5′-GAA GTA CTC ATA GGC ATT CTC TGC-3′; BAX β, 5′-CAG CTC TGA GCA GAT CAT GAA GAC-3′ and 5′-GCC CAT CTT CTT CCA GAT GGT GAG-3′; BAX δ, 5′-AGC TCT GAG CAG ATC ATG AAG AC-3′ and 5′-CAA AGT AGA AAA GGG CGA CAA C-3′; GADD34, 5′-GAT GAG GAA GAA GAT GAG GAC AGT-3′ and 5′-GAC TTC AAG AAG ACA CCT GTA GCA-3′; GADD45, 5′AGC AGT TAC TCC CTA CAC TGA TGC-3′ and 5′-CTG CAA AGT CAT CTA TCT CCG GGC-3′; TRAIL, 5′-CAG TCT CTC TGT GTG GCT GTA ACT-3′ and 5′-TAT GTG AGC TGC TAC TCT CTG AGG-3′; DR6, 5′-ACC TTC TCA GAT GTG CCT TCT AGT-3′ and 5′-CTA CAC GAG GCA GAA GAG TTG GAT-3′; TRAIL R3, 5′-TCA GAA CAT ACT GGA GCC TGT AAC-3′ and 5′-CAG GAC GTA CAA TTA CTG ACT TGG-3′; MDA7, 5′-TAA GCA GCG CCM GMT GAC AGT CAG-3′ and 5′-CAC ACT GTG GCA GGG ATT GTG AGG-3′; BCL-2, 5′-CTG TGG ATG ACT GAG TAC CTG AAC-3′ and 5′-AAC TGA GCA GAG TCT TCA GAG ACA-3′; BCL-2, 5′-CCT TCT TTG AGT TCG TGT GG-3′ and 5′-CAG CCA GGA GAA ATC AAA CAG AGG-3′; BCL-XL, 5′-TTG GAC AAT GGA CTG GTT GA-3′ and 5′-GTA GAG TGG ATG GTC AGT G-3′; CASP-1, 5′-AAC TTA ATA TGC AAG ACT CTC AAG-3′ and 5′-GCG GCT TGA CTT GTC CAT TAT TGG-3′; CASP-3, 5′-ATG GGA ACA CTG AAA ACT CAG-3′ and 5′-GTC ATC ATC AAC ACC TCA GTC T-3′; CASP-2, 5′-GTT ACC TGC ACA CCG AGT CAC G-3′ and 5′-GCG

TGG TTC TTT CCA TCT TGT TGG TCA-3′; IRF-1, 5′-ATT CAC ACA GGC CGA TAC AA-3′ and 5′-ACT ATG GAA GAG ACT ACC TGA-3′; IRF-2, 5′-ATC CAT ACA GGA AAG CAT CA-3′ and 5′-AAT CAT TAC CTC ATT CAC TA-3′; CASP-3, 5′-TGT TTC ATC CAG TCG CTT TG-3′ and 5′-ATT CTG TTG CCA CCT TTC GG-3′; CASP-7-RT, 5′-GGA GAA AGC TCA TGG CTG TGT-3′ and 5′-TCC5′-AAG CAA ACC TCG GGG ATA CT-3′; CASP-8-RT, 5′-AAG CAA ACC TCG GGG ATA CT-3′ and 5′-GGG GCT TGA TCT CAA AAT GA-3′; CASP-8-VC, 5′-ATT CAG CAA AGG GGA GGA GT-3′ and 5′-TGC ATC CAA GTG TGT TCC AT-3′; CASP-8-VD, 5′-GGA CTC TCC AAG AGA ACA GGA TAG-3′ and 5′-TCT ACT GTA CCT GCA TCC AAG TGT-3′; and CASP-8-VE, 5′-GAC TGG ATT TGC TGA TTA CCT ACC-3′ and 5′-ATG ACC CTC TTC TCC ATC TCT ATG-3′. Amplification was carried for 35 cycles (hot start 2 minutes at 95°C, 15 seconds at 95°C, 25 seconds at 54°C, and 25 seconds at 72°C). To determine the amplification efficiency of the target, serial dilutions of the samples were amplified, and the run was analyzed with light cycle software under conditions of a low error rate (<0.2). The formula (efficiency = $10^{-1/slope}$) was used, where slope was determined from standard curves. The specificity of the primers was determined by agarose electrophoresis of the PCR product. β-actin was used as the internal control, and leukemic K562 cells containing 1,544 copies of β-actin mRNA per cell (8) were used as standard to determine the approximate number of copies in the target gene.

Western Blot Analysis. Cultures used in this experiment were harvested at the same time intervals used for harvesting RNA. Cells were washed ($2\times$) with cold PBS and lysed (while still attached) for 30 minutes in 100 μL of ice-cold radioimmunoprecipitation assay buffer [50 mmol/L Tris-HCl (pH 8.0), 150 mmol/L NaCl containing 0.1% SDS, 1% NP40, 0.5% sodium deoxycholate, 0.1 mg/ml phenylmethylsulfonyl fluoride, 1 mmol/L sodium orthovanadate, and 1 mg/ml aprotinin]. Cell debris was removed by centrifugation at 14,000 $\times$ g for 10 minutes at 4°C. Protein was determined with the Bio-Rad protein assay (Bio-Rad Laboratories, Hercules, CA). Aliquots of cell extracts containing 50 μg of total protein were resolved by 10% SDS-PAGE and transferred to polyvinylidene difluoride membranes (Perkin-Elmer Life Sciences, Inc., Boston, MA). Filters were blocked for 1 hour at room temperature in Blotto A [5% nonfat dry milk powder in 1 M Tris (pH 7.4), 5 M NaCl, and 0.05% Tween 20] and then in Blotto A containing a 1:500 to 1:100 dilution of the following: (a) the rabbit polyclonal GADD45, GADD34, GADD153, and p-38 antibodies or the mouse monoclonal P-p38, p21, CDC2, and SMAD4 antibodies from Santa Cruz Biotechnology (Santa Cruz, CA); and (b) the rabbit polyclonal P-AKT(Ser473) and P-AKT(Thr308), P-Rb(Ser780), P-Rb-(Ser795), P-Rb (Ser807/811) or mouse monoclonal Rb antibodies from Cell Signaling Technology (Beverly, MA). After washing in 1 M Tris (pH 7.4), 5 M NaCl, and 0.05% Tween 20 buffer (4 $\times$ 10 minutes, reverse transcription), filters were incubated for 1 hour at room temperature in Blotto A containing 1:4,000 dilution of peroxidase-conjugated antirabbit secondary antibody (Amersham Biosciences Corp., Piscataway, NJ) or Blotto A containing 1:4,000 dilution of peroxidase-conjugated antimouse secondary antibody (Amersham Biosciences Corp.). After washing in 1 M Tris (pH 7.4), 5 M NaCl, and 0.05% Tween 20, enhanced chemiluminescence was done according to the manufacturer's recommendation. Protein expression was quantitatively analyzed via laser-scanning densitometry with NIH Image Version 1.61 software. All results were normalized to β-actin.

Activation Status of NF-κB Assessed by p65/p50 Localization with Double Immunofluorescence Assay. Cells were cultured on Lab-Tek chamber slides (Nunc Inc., Naperville, IL) under normal and methionine-stress conditions. Slides were blocked with 3% BSA in PBS (pH 7.4) with 0.25% Tween 20 for 30 minutes. Slides were then incubated overnight at 4°C in primary antibodies, mouse anti-p65 and rabbit p50 (Santa Cruz Biotechnology), diluted 1:100 with the blocking buffer. After washes in PBS (pH 7.4) with 0.25% Tween 20 (3 $\times$ 15 minutes), the cells were overlaid with secondary antibodies, Cy2-conjugated antimouse IgM and Cy3-conjugated antirabbit IgG, diluted 1:1000 in blocking buffer. After three washes in PBS (pH 7.4) with 0.25% Tween 20 (3 $\times$ 15 minutes) and one wash in PBS (1 $\times$ 15 minutes), the slides were mounted with aqueous mounting media with antifade and 4′,6-diamidino-2-phenylindole (VectaShield, Vector, Burlingame, CA) and visualized with a Zeis epifluorescence microscope.

RESULTS

Physiologic Response of CNS Tumors to Methionine Stress

Fig. 1 illustrates the response of the tumor cell lines DAOY, SWB77, SWB40, SWB39, and SWB61 to methionine-stress culture conditions. Replacement of methionine with homocysteine resulted in marked decrease of mitotic index in all of the cultures. Cell death was most prominent in SWB61 followed by DAOY, SWB40, SWB39, and SWB77, in which cellular death was protracted and sporadic. In contrast, the control 3T3 continued to proliferate in homocysteine (data not shown). Massive cell death was evident in SWB61 and DAOY after 2 days of methionine stress, whereas longer periods were required for SWB40 and SWB39 to respond. SWB77 overcame an initial mitotic arrest and, like the control 3T3 (not shown), it adapted to methionine stress assuming a different morphology. In addition to cell division, methionine stress inhibited cell migration and colony formation. Cell migration and colony formation were restored by replenishing methionine, and mitosis was evident in or near colonies but not in migrating single cells (Fig. 2). The effect of methionine stress on the cell cycle is shown in Table 1. SWB61 and DAOY displayed a marked G_1 arrest and a repression of the S phase after
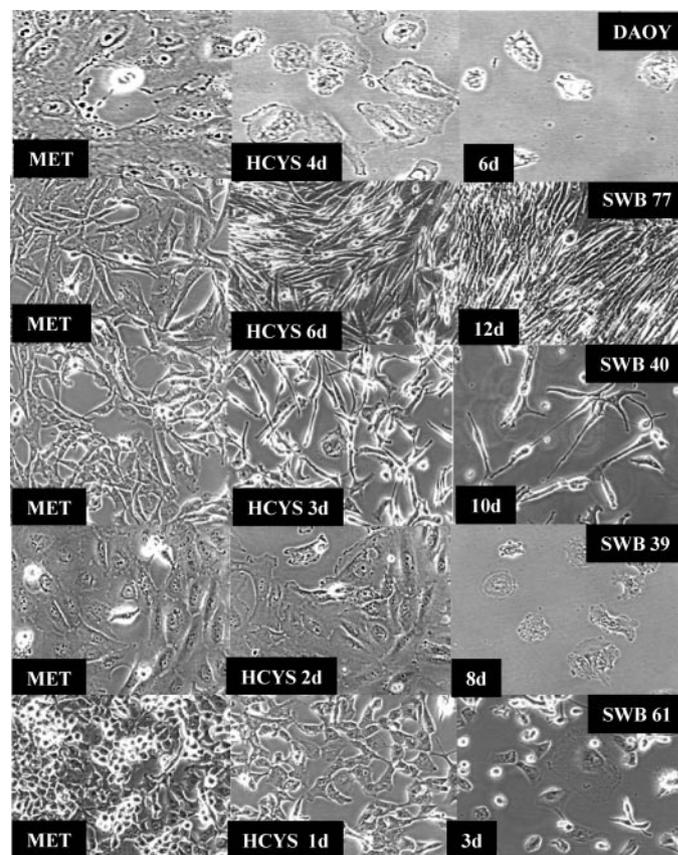

Fig. 1. The effect of methionine stress in DAOY, SWB77, SWB39, SWB40, and SWB61 shown from *top* to *bottom*. Culture conditions and duration of stress is shown at the *bottom* of each panel. Replacement of methionine with homocysteine in culture results in marked decrease of mitotic index in DAOY, SWB39, SWB40, and SWB61. Cell death was most prominent in SWB61 followed by DAOY, SWB40, SWB39, and SWB77, which was resistant to replacement of methionine with homocysteine. Massive apoptosis occurred in SWB61 and DAOY at days 2 and 4 after initiation of methionine stress, respectively, whereas longer time periods were required for SWB40 and 39 to be nearly eradicated. Note the intense mitotic activity in SWB61 growing in methionine medium and abolition of mitosis on replacement of methionine with homocysteine. Magnification $\times$400. (*HCYS*, homocysteine).
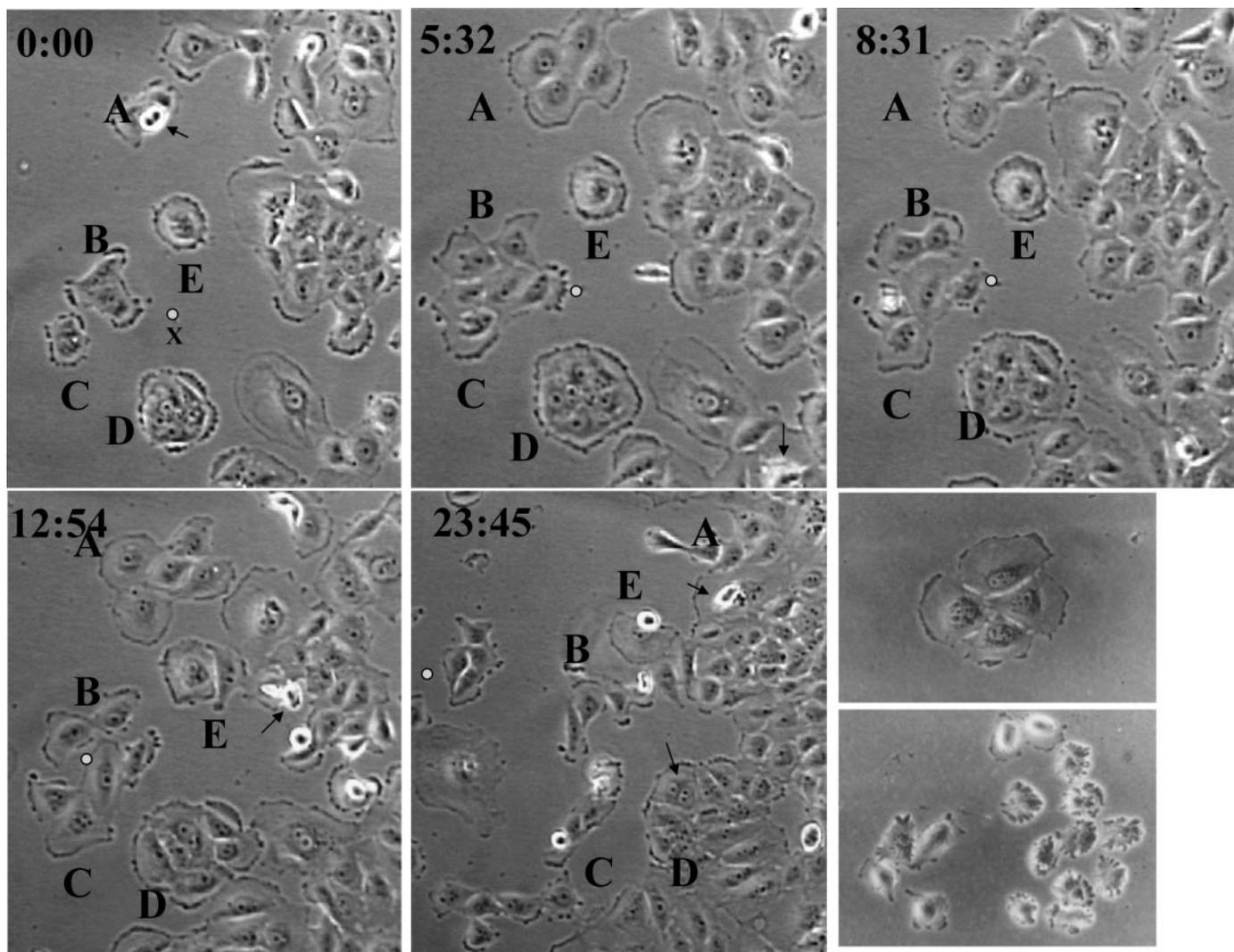
7515

Fig. 2. Recovery of motility, colony forming ability and mitotic activity in DAOY on replenishment of methionine in the culture medium. Two days after methionine restoration, the motility of clusters of DAOY cells was monitored for 24 hours during the third day. Motility of multinucleated cells or groups of cells (*A–E*) is shown in relation to the point of reference marked X. Mitosis is restored either when individual cells approach the colony or within the colony (*arrows*). Magnification ×100. Octaploid cells in G_2 separate and subsequently divide to yield single G_1 cells (*last panel*). Magnification ×250.

methionine withdrawal, respectively. SWB39 showed a G_2 arrest followed by a G_1 arrest after methionine withdrawal. SWB40 showed a S-phase increase concomitant with G_1 depletion after several days in methionine-void medium. The peak of cell cycle arrest coincided with increased apoptosis in all of the methionine-dependent lines tested, and such correlation was more pronounced in SWB61 and DAOY. The decline in tumor cell proliferation under methionine stress cannot be attributed to a single cell cycle block and may involve additional factors, such as failure to complete mitosis. The low mitotic index in methionine-stressed tumor lines combined with the decline of G_2 cells in DAOY (5 days), SWB61 (2 days), and SWB40 (4 days) indicate that these cells may die during an attempt to divide.

c-DNA Analysis

The relative gene expression in cell lines grown under control conditions or maintained under methionine stress for a period of time required to induce a peak of cell cycle arrest 24 hours before a sharp increase of the apoptotic index (Table 1) was determined by c-DNA array analysis. Genes, the expression of which was significantly changed ($P > 0.05$; see supplement), were classified based on their function, such as cell cycle related, p53 related, related to apoptosis/antiapoptosis, growth factor/angiogenesis related, cytokine dependent, and so forth.

DAOY Medulloblastoma

The most notable changes in gene expression induced by methionine stress in DAOY are described below.

Cell Cycle Related. Down-regulated: cyclins A1 (×2.6), A2 (×2.2), B1 (×2.1), B2 (×2.9), D2 (×1.8), CDC2 (×2.8), CDC25A (×1.9), and B (×2.0), proliferating cell nuclear antigen (PCNA; ×1.5), E2F-4 transcription factor (×1.4), and CDC2-related protein kinase (×1.4); and up-regulated: Cyclins D1 (×3.9) and D3 (×2.1) and cyclin-dependent kinase (CDK)6 (×6.6).

Mitosis Related. Up-regulated: MAD1 (×2.7), CDC5L (×1.4), and CDC14A2 phosphatase (×5.9); and down-regulated: BUB1 (×2.0) and 3 (×1.3), MAD2 (×2.0), CKS1 (×2.0), CDC20 (×2.6), and NET1 (×2.2).

Cell Cycle Inhibition and Checkpoint Related. Up-regulated: p21 (×2.9), SKP1 (1.6), GADD34 (×3.4), GADD45α (×3.1), BRCA-1 (×1.9), 14-3-3σ (×1.6), and GADD45γ (×53).

7516

Table 1 *Flow-cytometric cell cycle analysis and apoptotic index of CNS tumor cells in MET and HCYS media. The apoptotic index represents the average number of cells dying per two-day interval under steady state culture in HCYS and expressed as percent of living cells in the culture*

Cell (media)	Days in HCYS	G_1 (%)	G_2 (%)	S (%)	Effect	Apoptosis % (2d)
SWB61 (MET)		45–30*	6–14	49–57		28
(HCYS)	1	79†	1	20	G_1/S arrest‡	36
	2	77	3	20	G_2 and mitosis reduced	51§
	3	74	4	22	Apoptosis in G_1	57
DAOY (MET)		67–55	8–15	25–30		10
(HCYS)	2	76	9	15	G_1/S arrest	28
	4	68	14	18	G_2-phase depleted	61§
	6	85	2	12	Motility inhibited	66
	8	88	1	11		
SWB40 (MET)		86–83	3–9	7–11		4
(HCYS)	2	81	8	12	G_2 arrest	11
	4	79	1	21		22
	8	62	6	32		28§
	12	66	6	28		43
SWB39 (MET)		87–69	3–6	10–24		7
(HCYS)	2	55	13	30	G_2 arrest	10
	4	60	7	34		26
	6	66	14	19	G_2-phase depleted	55§
	8	82	5	13	Motility inhibited	64
	10	83	6	11		
SWB77 (MET)		91–84	4–9	5–10		8
(HCYS)	2	92	6	2	No effect	15
	6	92	6	2		20
	10	88	9	3		23
NIH-3T3 (MET)		93–90	1–3	5–9		5
(HCYS)	10	96–93	1–3	3–4	No effect	4

Abbreviations: HCYS, homocysteine; MET, methionine.
* Range from three determinations.
† Mean of three determinations.
‡ Most likely event in response to MET-stress.
§ Denotes the onset of increased apoptosis.

Apoptosis Related. Up-regulated: BCL1 ($\times$4), BCL-2 interacting killer (BIK; $\times$2), TRAIL ($\times$32), TRAIL-R2 ($\times$1.9), and DR6 ($\times$43).

Tumor Necrosis Factor (TNF)-α Related. Up-regulated: TNF-α ($\times$1.7), TRADD ($\times$8.5), TRAF-interacting protein (I-TRAF; $\times$3.1), and TNFSF10 ($\times$36); and down-regulated: inhibitor of apoptosis protein (IAP)-β.

Cytokines. Induced or up-regulated: IL-24 (MDA7 or ST16) ($\times$89), SCYA20 ($\times$322), SCYA7 ($\times$11), interleukin (IL)-1B ($\times$24), IL-1A ($\times$25), IL-6 ($\times$24), IL-8 ($\times$80), SGRF ($\times$5.1), IL-11 ($\times$7.4), IL-1R type I ($\times$7.5), and type II ($\times$7.2).

IL-Related. Down-regulated: IL-1 signaling factors Tollip-like receptor (TLR)3 ($\times$5.3), interleukin receptor-associated kinase (IRAK; $\times$1.7), TAB1 ($\times$2.5), and myeloid differentiation primary response protein (MyD88; $\times$1.9); and up-regulated: IL-1B converting enzyme γ ($\times$2.3), δ ($\times$3.0), ϵ ($\times$27.4), ICE ($\times$26), and MAP kinase kinase (MKK)3 ($\times$2.1).

Interferons. Induced or up-regulated: IFN-α ($\times$4.1), IFN-β ($\times$73), IRF1 ($\times$4.8), IRF3 ($\times$2.2), IRF7 ($\times$1.7), IFN-inducible protein kinase (PKR; $\times$2.1), IFN-γ receptor α chain ($\times$2.1), IFN-γ receptor I ($\times$1.7) and II ($\times$2.1), IFN-γ-inducible indoleamine-dioxygenase (IDO; $\times$3.6), IFN-γ inducible protein (IP-30; $\times$1.9), IFN-induced transmembrane protein II ($\times$2.1), IFN-γ–inducible mRNA ($\times$3.9), and ISG15 ($\times$6.9).

Insulin Related. Down-regulated: IGF2 ($\times$2.3) and IGFBP5 ($\times$8.3); and up-regulated: IGFBP4 ($\times$1.9) and IGFBP7/mac25 ($\times$54).

TGF-β Related. Up-regulated: TGF-β ($\times$3.8) and the inducible early growth response protein α (TIEG; $\times$3.2); and down-regulated: TAK1 ($\times$16.7).

Transcription Factors. Up-regulated: NF-κB p50 ($\times$2.8), JUN-B ($\times$4), c-JUN ($\times$3.9), plasminogen activator inhibitor (PAI)2 (6.6), and c/EBP-β ($\times$1.9); and down-regulated: c-FOS ($\times$2).

Miscellaneous. Down-regulated: topoisomerases II ($\times$2) and III ($\times$1.5), thymidine kinase ($\times$1.6), MAP4 ($\times$2), stathmin ($\times$1.8); and

up-regulated: integrin ($\times$2.0), inositol 1, 4, 5-triphosphate receptor type I ($\times$4.4), and adrenomedullin ($\times$5.1).

SWB61 Oligodendroglioma

Cell Cycle Progression and Checkpoint Induction. Up-regulated: p53 ($\times$4.7), p21/Waf-1 ($\times$2.6), GADD45α ($\times$3.7), BRCA1 ($\times$3.3), GADD34 (8.3), 14-3-3 η ($\times$1.4), ϵ (x7.3), σ (x1.6), cyclin D1 ($\times$2.5) and D3 ($\times$2.9), CDK4 ($\times$6.1), and SKP1 ($\times$1.7); down-regulated: CDC25B ($\times$1.8), cyclins A1 ($\times$4), A2 ($\times$2.2), B1 ($\times$7.1), and B2 ($\times$5.3), CDC2 ($\times$2.3), and its kinase ($\times$1.7), CDC25B ($\times$1.8), ASK (2.6), and DNA polymerase α ($\times$7.1).

Mitosis Related. Up-regulated: CDC5L ($\times$1.3), MAD1 ($\times$1.7), tumor endothelial marker precursor (TEM)1 (2.4), and CDC5L (1.3); and down-regulated: MAD2 ($\times$1.5), CDC14B ($\times$4), and BUB1 (2.6).

Apoptosis. Up-regulated: BCL-1 ($\times$15), BAX δ ($\times$21), NIP3 ($\times$2.7), TRAIL ($\times$5.5), TRAIL-R 2 ($\times$2.9), and DR6 ($\times$8.6); and down-regulated: BCL-2 ($\times$5).

TGF-β Related. Up-regulated or induced: TGF-β ($\times$13), β2 ($\times$3), TIEG ($\times$40), TGF-β receptor associated protein 1 ($\times$4.5), SMAD5 ($\times$2.6), SMAD2 ($\times$10), JUN-B ($\times$20), and tissue inhibitor of metalloproteinases (TIMP; $\times$31); and down-regulated: activin receptor-like kinase 4 (ALK4; $\times$4), TAK1 ($\times$2.8), SMAD3 ($\times$2), TIAF ($\times$2.3), c-FOS ($\times$3.0), MMP1 ($\times$6.7), and phospholipase c ($\times$7.7).

Insulin Related. Down-regulated: IGF-2 ($\times$5.9); and up-regulated: IGFBP6 ($\times$8.8) and IGF-2R ($\times$2.3).

TNF-α Related. Down-regulated: TNF-α ($\times$10) and TRADD ($\times$1.8); and up-regulated: TACE ($\times$3.5), TRAF-2 ($\times$6.3), TRAF-6 ($\times$6.1), I-TRAF ($\times$2.4), and TNF-R2 ($\times$1.7).

Cytokine Related. Down-regulated: IL-1B ($\times$4.4), IL-11 ($\times$2.3), IL-10 ($\times$10), IL-13 ($\times$12), IL-4 ($\times$4.4), IL-8 ($\times$1.6), the receptors IL-1R2 ($\times$3.5), IL-8RB ($\times$3.9), IL-5RA ($\times$9.1), IL-10R ($\times$20), IL-

7517

11RA ($\times$16.7), IL-9R ($\times$6.7), TAB ($\times$3.3), and Tollip ($\times$100); and up-regulated: IL enhancer binding factor 3 ($\times$2.8), TACE ($\times$6.1), IRAK ($\times$2.1), NIK ($\times$9.4), MyD88 ($\times$5.8), Iκ kinase (IKK)-α ($\times$1.4), and IKB-ϵ ($\times$2).

Interferons. Up-regulated: IRF1 ($\times$5.1), IRF3 ($\times$3), IRF5 (3.1), and IRF7 (1.7), the IFN-γ–receptor α chain ($\times$2.9), IP-3 ($\times$2.1), AF-1 ($\times$3.1), FRD1 ($\times$3.9), growth-arrest-specific protein (GAS; $\times$4.1), and ISG-15 ($\times$2.8); and down-regulated: IFNα ($\times$25), ISG3 ($\times$1.3), IRF2 ($\times$1.4), IRF6 ($\times$6.7), and PKR ($\times$2.7).

Transcription Factors. Down-regulated: extracellular signal-regulated kinase (ERK1; $\times$1.6), ELK1 ($\times$2), R-kB ($\times$3.5), cAMP responsive element-binding protein (CREB; $\times$2.5), ELK1 ($\times$1.7), PAI2 ($\times$5), and c-FOS ($\times$3.0); up-regulated: NF-κB p50 ($\times$15), p65 ($\times$3.8), JUN-D ($\times$1.6), JUN-B (19.7), c-JUN ($\times$6.9), v-Fos transformation effector (FTE)1 ($\times$2.9), B-cell translocation gene (BTG)1 ($\times$3.1), PC4 ($\times$3.9), ERK3 ($\times$2.1), ELK3 (10.3), PAI1 (3.6), c/EBP-β ($\times$3.6), c-EBP-γ ($\times$3.2).

Miscellaneous. Down-regulated: phospholipase c (7.7), MAP4 ($\times$1.9), separatin ($\times$3.6), topoisomerase I ($\times$3.0), and II ($\times$3.6); and up-regulated: integrin ($\times$1.4) and adrenomedullin ($\times$3.2).

SWB40 Astrocytoma

Cell Cycle Related. Down-regulated: cyclins A1 ($\times$3.6), A2 ($\times$2.9), B1 ($\times$8.3), B2 ($\times$5.3), D3 ($\times$1.5), CDC2 ($\times$2.4), CDK5 ($\times$1.6), CDK6 ($\times$2.6), CDK4 ($\times$4.3), SKP1 ($\times$1.6), CDC25A ($\times$1.5), and B ($\times$4.0), and DNA polymerase α ($\times$2.5); and up-regulated: cyclins D1 ($\times$5.5).

Mitosis Related. Up-regulated: MAD1 ($\times$1.6) and CDC5L ($\times$1.2); and down-regulated: BUB1 ($\times$12.5), BUB3 ($\times$1.8), MAD2 ($\times$2.0), CKS1 ($\times$1.5) and 2 ($\times$2.1), CDC20 ($\times$4.6), CDC14A2 phosphatase ($\times$3.0), and NET1 ($\times$2.0).

Cell Cycle Inhibition and Checkpoint Related. Up-regulated: p21 ($\times$2.7), GADD34 ($\times$3.2), GADD45α ($\times$1.4), BRCA1 ($\times$1.4), 14-3-3σ ($\times$1.6), and GADD45γ ($\times$2.1).

Apoptosis Related. Up-regulated: BCL-1 ($\times$2.8), BAX δ (2.1) and β ($\times$2), TRAIL-R2 ($\times$3.6), and DR6 ($\times$2.6); and down-regulated: BCL-2 ($\times$2.0) and IAP-β ($\times$2).

TNF-α Related. Down-regulated: TNF-R2 ($\times$1.4); and up-regulated: TACE ($\times$1.8) and I-TRAF ($\times$2.4).

Cytokines. Up-regulated: IL-8 ($\times$15) and the interleukin 13 receptor IL-13R ($\times$2.4).

IL Related. Down-regulated: IRAK1 ($\times$1.3), TAK-1 binding protein (TAB-1; $\times$1.9), and MyD88 ($\times$2); and up-regulated: IL-1B converting enzyme γ ($\times$2.1), IKB-ϵ ($\times$2), and NIK ($\times$1.8).

Interferons. Induced or up-regulated: IFN regulatory factors 1 (IRF-1; $\times$2.4), IRF-5 ($\times$1.7), and IRF-7 ($\times$69), IFN-inducible protein kinase (PKR; $\times$1.9), IFN-γ as reflected by up-regulation of IFN-γ–receptor α chain ($\times$1.6), FRD1 ($\times$3.2), and IFN-γ–inducible protein (IP-30; $\times$1.4).

Insulin Related. Down-regulated: IGFBP4 ($\times$4.0), IGFBP6 ($\times$2.4), and IGFBP5 ($\times$2.5); and up-regulated: IGF-2R ($\times$1.8).

TGF-β Related. Up-regulated: TGF-β ($\times$11), TIEG ($\times$7), and SMAD5 ($\times$2); and down-regulated: TAK1 ($\times$1.4) and SMAD6 ($\times$4.0).

Transcription Factors. Up-regulated: JUN-D (1.7), FTE1 (1.6), BTG1 ($\times$2.3), PC4 ($\times$3.2), CREB ($\times$2.0), c/EBP β ($\times$2.2) and γ ($\times$5.6), and ERK3 ($\times$1.5); and down-regulated: c-JUN ($\times$1.3), JUN-B ($\times$4), ERK1 ($\times$1.7), and c-FOS ($\times$5).

Miscellaneous. Down-regulated: topoisomerase II ($\times$2), dehydrofolate reductase ($\times$6.7), thymidine kinase ($\times$3.9), adrenomedullin (1.6), MAP4 ($\times$1.5), and stathmin ($\times$2.3); and up-regulated: inositol 1, 4, 5-triphosphate receptor type I ($\times$23) and integrin ($\times$1.5).

SWB39 Glioblastoma Multiforme

Cell Cycle Related. Down-regulated: cyclins A2 ($\times$5.6), B1 ($\times$2.7), B2 ($\times$4.6), and D3 ($\times$1.7), CDC2 ($\times$2.3), CDK6 ($\times$1.9), CDC25A ($\times$2) and B ($\times$1.8), and CDC2-related protein kinase ($\times$1.5); and up-regulated: cyclins D1 ($\times$1.2).

Mitosis Related. Up-regulated: MAD1 ($\times$2.4) and CDC5L ($\times$1.2); and down-regulated: BUB1 ($\times$3.5) and 3 ($\times$1.9), MAD2 ($\times$2.9), CDC28 kinase (CKS2; $\times$1.6), and CDC20 ($\times$2.1).

Cell Cycle Inhibition and Checkpoint Related. Up-regulated: p21 ($\times$2.1), GADD34 ($\times$2.3), GADD45α ($\times$2.4), BRCA1 ($\times$2.4), BRCA2 ($\times$3), 14-3-3 ϵ ($\times$2.3), and GADD45γ ($\times$6.1); and down-regulated: p53 binding protein ($\times$2.9) and SKP1 ($\times$2.3).

Apoptosis Related. Up-regulated: BCL1 ($\times$1.4), NIP3 (5.5), TRAIL ($\times$7), TRAIL-R2 ($\times$2), and DR6 ($\times$3.7); and down-regulated: IAP-β ($\times$2).

TNF-α Related. Up-regulated: TRADD ($\times$11), I-TRAF ($\times$3.6), and TNFSF10 ($\times$1.8); and down-regulated: TNF-R2 ($\times$1.5).

Cytokines. Induced or up-regulated: IL-24 (MDA7 and ST16) ($\times$21), SCYA20 ($\times$320), IL-1A ($\times$3.3), IL-6 (7.3), IL-8 terminal variant ($\times$6.4), and the interleukin receptors IL-1R type I ($\times$4.0).

IL-Related. Down-regulated: IRAK ($\times$2.1); and up-regulated: IL-1B converting enzyme γ ($\times$2.3), δ ($\times$3.3), ϵ ($\times$2.9), and IKB ϵ ($\times$1.6).

Interferons. Induced or up-regulated: IRF-1 ($\times$1.8), IRF-3 ($\times$2.1), IRF-5 (1.7), IRF-7 (2.5), GAS ($\times$2), IFN-γ receptor I ($\times$1.6), and ISG15 ($\times$4.5); and down-regulated: IRF 6 ($\times$1.9), IFN-inducible peptide ($\times$16.7), and IFN-inducible protein kinase (PKR; $\times$2.6).

Insulin Related. Down-regulated: IGFBP-6 ($\times$1.5); and up-regulated: IGF-2R ($\times$1.5) and IGFBP4 ($\times$1.8).

TGF-β Related. Up-regulated: TGF-α ($\times$5.5), TGF-β ($\times$6.6) and of the inducible early growth response protein α (TIEG; $\times$2.7), and TMP (2.2); and down-regulated: TGF-β2 ($\times$2.2) and TAK1 ($\times$2.0).

Transcription Factors. Up-regulated: NF-κB p50 ($\times$1.6), p65 ($\times$1.5), BTG1 ($\times$2), PC4 ($\times$1.3), CREB ($\times$2) and c/EBP-β ($\times$2.4); and down-regulated: JUN-B ($\times$3.1) and ELK1 ($\times$1.5).

Miscellaneous. Down-regulated: topoisomerase II ($\times$2.7) and III ($\times$1.5), stathmin ($\times$1.8); and up-regulated: inositol 1, 4, 5-triphosphate receptor type I ($\times$2.4), BCL-6 ($\times$2), and adrenomedullin ($\times$2.3).

SWB77 Glioblastoma Multiforme

Cell Cycle Related. Down-regulated: cyclins A2 ($\times$1.9), D1 ($\times$1.5), CDC2 ($\times$1.3), CDC25A ($\times$3.3), and CDC25B ($\times$1.5); and up-regulated: cyclins D2 ($\times$2.3) and D3 ($\times$2.4).

Mitosis Related. Down-regulated: MAD1 ($\times$3.5) and CDC20 ($\times$1.8).

Cell Cycle Inhibition and Checkpoint Related. Up-regulated: GADD45α ($\times$1.4) and BRCA-1 ($\times$2.1); and down-regulated: p21 ($\times$2.3), E2F-4 ($\times$1.4), and 14-3-3 σ ($\times$1.4).

Apoptosis Related. Down-regulated: TRAIL-R2 ($\times$1.6).

TNF-α Related. Up-regulated: TRADD ($\times$1.7).

Cytokines. Down-regulated: IL-11 ($\times$5.9).

Interferons. Induced or up-regulated: IFN-γ–receptor α chain ($\times$2.6), IP-30 ($\times$1.7), and FRD1 ($\times$1.8).

TGF-β Related. Up-regulated: TGF-β ($\times$1.4) and TGF-β–activated kinase 1a ($\times$1.6); and down-regulated: TIEG ($\times$3.1).

Transcription Factors. Up-regulated: JUN-D ($\times$1.4), FTE1 ($\times$1.4), and PC4 ($\times$1.8).

Miscellaneous. Up-regulated: inositol 1, 4, 5-triphosphate receptor type I ($\times$16) and adrenomedullin ($\times$2.9); and down-regulated: topoisomerase II ($\times$10) and III ($\times$1.3).

7518

Table 2 *Verification of microarray data by real-time PCR.*

Cell line culture condition	DAOY		SWB61		SWB40		SWB39		SWB77	
	MET	HCYS	MET	HCYS	MET	HCYS	MET	HCYS	MET	HCYS
Gene	Number of copies per cell									
DR6	**0.9***	**21**	**1.5**	**6.9**	**3.6**	**21**	**2.4**	**10.5**	**3.1**	**1.3**
IkBe	6.6	8.4	**9**	**17.7**	**0.2**	**6**	**12.1**	**19.8**	**0.6**	**1.5**
NFkB (65)	15.3	18.4	**10**	**24**	**15**	**33**	**21**	**45**	19.3	18
NFkB (50)	**6**	**18**	**1.5**	**14.5**	4.4	6	**12.1**	**30**	**0.6**	**2.1**
NFkB	**15.3**	**29.7**	30.2	34.5	14.3	15.9	31.3	31.8	18.3	14.1
RkB	14.3	14.6	**36.4**	**12.5**	14.3	15	8.7	6.2	15	14
BAK	**0.51**	**1.8**	**0.24**	**0.9**	3.9	3.6	**3**	**1.5**	6.6	6.3
BAX (δ)	7.5	6.6	**0.75**	**9**	**3.3**	**9**	**11.5**	**15.8**	6.2	7.5
BAX (β)	7.5	6.6	**14.4**	**8.4**	**4.5**	**15.8**	9.9	12.2	**0.15**	**0.18**
BCL2	5.1	4.5	**7.2**	**1.4**	**7.5**	**4.5**	0.3	0.2	2.4	1.4
GADD34	11.8	33.2	12.3	27.1	13.8	60	21.7	45.5	2.7	1.4
TRAIL	**0.9**	**26.0**	4.4	4.8	5.4	4.4	**1.6**	**6.8**	0.3	0.6
TRAILR3	4.8	4.5	0.02	0.03	**0.06**	**0.45**	0.6	0.16	**0.03**	**0.1**
BCL-XL	**3**	**6.6**	9.0	7.7	6.1	6.0	6.0	7.7	4.5	4.2
IRF-1	**1.8**	**12**	**2.4**	**7.8**	**4.4**	**14.8**	**15.4**	**24.15**	6.0	6.0
IRF-2	**7.4**	**2.8**	**5.1**	**3.0**	4.6	4.6	6.6	6.9	6.0	4.5
CASP-1	**0.28**	**6.5**	0.12	0.3	**0.45**	**3.6**	3.1	1.4	0.45	0.6
CASP-2	**3.0**	**4.8**	6.0	5.7	**16.0**	**30.2**	18	15	3.2	3.0
CASP-3-RT	0.45	4.4	0.75	0.28	1.4	2.8	1.5	0.6	0.21	0.18
CASP-7-RT	**0.15**	**0.64**	0.24	0.24	0.9	2.8	1.6	0.92	**0.14**	**0.75**
CASP-8-RT	**3.9**	**14.5**	9.0	4.5	12	27	30	24	1.2	1.8
CASP-8-VC	**3.9**	**16.3**	9.0	3.9	12	27	30	24	**1.43**	**6**
CASP-8-VD	**1.8**	**9.1**	6.0	3.0	9.0	21	16.5	24	0.47	1.4
CASP-8-VE	**6.3**	**21**	17	6.1	18	44	3	45	1.55	3.0

NOTE. Bold = statistically significant changes in gene expression between MET and HCYS grown cells ($P < 0.05$).

Abbreviations: MET, methionine; HCYS, homocysteine.

* Number of RNA copies mean of SD from 5 determinations. RNA concentrations were determined from the number of cycles required to achieve a 30% of the maximum CYBR green fluorescence for each of the primers used in combination with 5 concentrations of cDNA preparations from each cell line, with standard plots of the log of β-actin copies *versus* cell cycle number for actin amplification to the same level. Copies of β-actin per cell for each cell line were determined by comparing the number of cycles required for similar signal actin amplification between cDNA preparations from the chronic myeloid leukemic K562 cells (known RNA copies) and unknowns from each of the above lines. Such comparisons require similar efficiency of cDNA amplification.

Validation of Affymetrix Chip Hybridization (Quantitative Real-Time PCR). Validation of Affymetrix chip hybridization was done with real-time PCR for several genes of interest, and expression was determined in comparison to β-actin (Table 2). There was a 94% agreement with the cDNA microarray analysis. According to reverse transcription-PCR data, TRAIL was up-regulated only in SWB39 and DAOY, whereas TRAIL-R3 was up-regulated in SWB40. BCL-XL was up-regulated in DAOY. Expression of p50-NF–κB and NF-κB–R were markedly up-regulated in DAOY, SWB61, and SWB39 by methionine stress. Examination of levels of expression of caspases (not provided by Affymetrix hybridization chip) indicated up-regulation of caspase 1 in DAOY and SWB61 and of caspase 2 in SWB40 by methionine stress, whereas caspase 3 was expressed marginally in all of the tumors and was modestly up-regulated only in DAOY under methionine stress. Similarly, robust up-regulation of caspase 8 was observed in DAOY and SWB40, whereas its expression was down-regulated in SWB61 and SWB39 under methionine stress. One of the genes that were strongly affected by methionine stress was the tumor suppressor/cytokine MDA7 (also known as IL-24). In accordance with c-DNA oligoarray analysis, low levels of MDA7 expression were present in all of the CNS tumors tested; however, substantial up-regulation by methionine stress occurred in DAOY and SWB39 and to a lesser extent in SWB40 and SWB61 (Fig. 3). No MDA7 signal was detected in the methionine-resistant SWB77 (Fig. 3). MDA7 mRNA levels increased progressively to reach maximum expression at days 6 to 8 in DAOY. Replenishing methionine resulted in down-regulation and loss of signal (at day 2). Relative ratios of MDA7 to actin were <0.005, 0.08, 0.21, and 0.30 at days 0, 2, 4, and 6, respectively, illustrating the rapid and substantial (>60-fold) increase.

Validation by Western Blot Analysis. Induction of MDA7 mRNA expression by methionine stress resulted in the synthesis of MDA7 protein in DAOY and SWB39 with concomitant activation of p38 (Fig. 4; Table 3). Although low levels of MDA7 mRNA were observed in SWB61 and SWB40, protein was not detectable by Western blot analysis. Induction of MDA7 protein in DAOY and SWB39 was accompanied by phosphorylation of p38, with no increase in total p38 expression. In contrast, p38 activation was inhibited in methionine-resistant SWB77. An increase ($P < 0.05$) in GADD45 protein was observed in DAOY under methionine stress. GADD45 protein was more pronounced in p53-efficient tumors SWB61 and 40 and to a lesser extent in mut p53 SWB39, indicating that GADD45 induction is p53 dependent. GADD34 was markedly up-regulated in SWB61 and to a lesser extent in SWB40, DAOY, and SWB39. Similarly, methionine stress resulted in the increase of p21 protein levels in all of the lines except in SWB77. The p21 synthesis
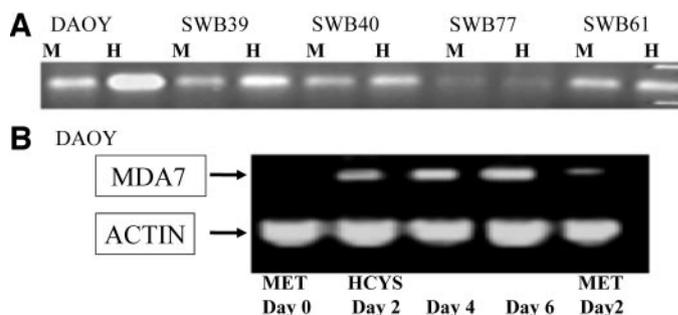

Fig. 3. *A.* Induction of MDA7 signal in CNS tumors in HCYS medium (*H*). Note that induction occurs in DAOY, SWB39, and to some extent in SWB61 and in SWB40. However, the signal is weak in SWB77 regardless of culture conditions. *B.* Time course of induction of MDA7 signal in DAOY: DAOY cells were cultured for 2 (*lane b*) or 4 (*lane c*) or 6 days (*lane d*) in HCYS and then returned to methionine media where they were allowed to enter G₁ and divide (*lane e*). Reverse transcription-PCR amplification of cDNA was done with the forward primer (5′TAA GCA GCG CCG TGA CAG TCA GG3′) and reverse primer (5′CAC ACT GTG GCA AGG ATT GTG AGG3′) to yield a fragment of 200b. β-actin is shown indicating equal loading. (MET, methionine; *HCYS*, homocysteine).

7519

Fig. 4. Effect of methionine stress on MDA7, P-p38, p53, p21, CDC2, SMAD4, Rb and phosphor-Rbs, and AKT inactivation/activation in response to methionine stress. Western blot analysis was done on whole cell lysates of CNS tumor cells growing in methionine-efficient medium under exponential growth or in resting cells under methionine-stress conditions 24 hours before the onset of massive apoptosis. MDA7 protein was synthesized under methionine stress in three of nine tumor lines tested, including DAOY and SWB39. Significant up-regulation of p38-phosphorylation under methionine stress was observed in the above two lines but not in SWB61, SWB40, or SWB77. Activation of p38 followed a time course parallel to that of MDA7 induction and reached a zenith 4 days after initiation of methionine stress (Table 2). Expression of p53 protein was up-regulated by methionine stress in SWB77, SWB61, and DAOY; however, up-regulation of p21 was evident in DAOY and to some extent in all of the other cell lines with the exception of SWB77, in which p21 was not synthesized under any of the conditions tested. CDC2 protein was down-regulated to nearly 50% of its baseline value in SWB40, SWB61, and DAOY and to a lesser extent in SWB39. A substantial increase of SMAD4 was observed only in DAOY. Synthesis of SMAD4 was markedly reduced in all of the other lines. High P-AKT levels decline in DAOY and SWB77 under methionine stress, indicating down-regulation of a robust PI3K/AKT pathway. Rb inactivation and subsequent cell cycle progression requires phosphorylation by cyclin D/CDK4, 6 (ser 780), and then by cyclin E/CDK2. Full activation of the AKT protein requires phosphorylation at Ser473 and Thr308. Rb and its phosphorylated forms are severely suppressed by methionine stress, however, hyperphosphorylated Rb is not detectable in DAOY and SWB61, whereas P-Rb (ser780) remains relatively high.
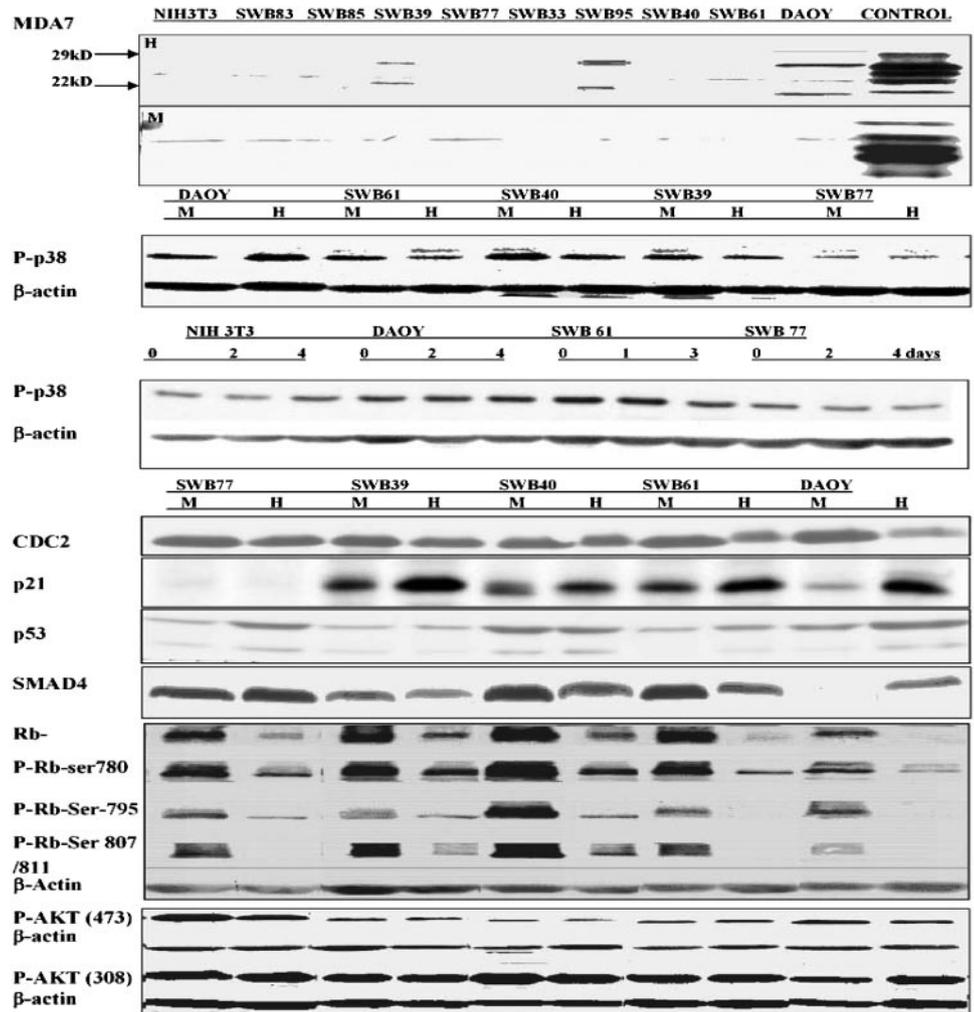
was induced by methionine stress regardless of p53 status and was pronounced in SWB61 (wt p53), DAOY, and SWB39 (mut p53). In contrast to MDA7 and the GADDs, the Rb protein and its phosphorylated forms were substantially suppressed (Table 3; Fig. 4). In methionine medium, levels of unphosphorylated Rb were high in SWB61 and 40 and less abundant in the glioblastoma multiformes SWB77 and 39, whereas such levels were markedly lower in DAOY. Under methionine stress, unphosphorylated Rb accumulated in all of the cell lines compared with its hyperphosphorylated form in the following order: DAOY = SWB61>SWB39>SWB40>SWB77. Methionine stress reduced phosphatidylinositol 3′-kinase (PI3k)/AKT phosphorylation at ser 473 and 308 in DAOY, SWB40, and SWB77; however, phosphorylation of AKT under methionine-stress conditions was more prominent in SWB77 than in all of the other tumors examined, regardless of culture conditions. Examination of the Affymetrix array data and the protein levels determined in this study suggests that RNA levels reflect protein synthesis in some cell lines but not in all of them. A reason for such discrepancy is not fully understood, but in this case it may be because of measuring gene expression and protein levels at the same time point. Therefore, it is possible that protein synthesis in response to RNA changes was occurring but had not reached its zenith at the time the measurement was made. In this regard small changes in protein levels between controls and methionine-stressed lines should not be disregarded, as they may increase in magnitude with time.

NF-κB Inactivation by Methionine Stress. Active NF-κB, as determined by colocalization of NF-κB subunits p50 and p65 in the nucleus, was observed in all of the cell lines tested and in SWB77 in particular (Fig. 5). Methionine withdrawal resulted in the failure of NF-κB subunits to enter the nucleus in SWB61 and DAOY. Methionine stress increased accumulation of NF-κB subunits in the cytosol. These findings strongly suggest that methionine stress causes substantial inhibition of NF-κB activity.

DISCUSSION

Methionine stress induces an arrest in cell proliferation with concomitant cell cycle blocks and induction of cell death, loss of motility, and failure to form colonies. These antitumor phenotypes are related to a range of altered signaling mechanisms. Although functional studies are required to pinpoint the exact pathways mediating the responses to methionine stress, the work presented here provides a comprehensive overview of the patterns of gene regulation in response to methionine stress. The major signal transduction pathways in CNS tumors that are affected by methionine stress and differences among CNS tumors in response to such stress are classified below.

Cell Cycle Control. Up-regulation of TGF-β by methionine stress in all of the methionine-dependent tumors tested coupled with the induction of p53 and GADD45 in p53-competent tumors inhibits early progression through G_1. Both the G_1 to S and the G_2 to M transitions are blocked by the up-regulation of p21 (9, 10). Up-regulation of BRCA1 and 14-3-3σ is also expected to exert an inhibitory effect on G_2-M progression of cell cycle, regardless of p53 status, by binding to phosphorylated CDC25. Down-regulation of CDC2 expression by

Table 3 *Western blot analysis of the MDA-7 and MDA-7-dependent proteins induced under methionine stress*

Tumor	Medium	MDA-7	p53	p21	p-38	P-p38	GADD45	GADD34	CDC2	SMAD4	P-AKT*	Rb	P-Rb†	Rb/P-Rb‡
							Density (% of actin)							
MET-dependent lines														
Daoy	M-	ND	63	7	45	24	11	24	310	12	152 (57)	24	68/49/45	0.5
Mut-p53	H48	5		93	41	33	21	33						
	H96	89		110	21	42	24	45						
	H144	112	130	165	13	52	24	84	110	53	77 (57)	6	14/4/2	3
SWB61	M-	ND	31	46	5	52	46	24	325	204	77 (61)	64	129/25/64	1
Wt-p53	H48	ND		180	5	46	158	34						
	H96	ND	68	391	5	45	194	56	115	104	75 (67)	15	31/4/3	3
	H144	ND				6	39	198	69					
SWB40	M-	ND	100	97	33	48	18	44	224	245	49 (144)	45	96/49/96	0.5
Wt-p53	H96	ND		145	32	33	54	68						
	H144	ND	76	145	35	23	67	98	116	135	18 (102)	11	55/12/5	2
SWB39	M-	ND	24	127	43	38	11	43	224	101	31 (54)	29	31/13/60	0.5
Mut-p53	H96	32		216	42	46	19	64						
	H144	66	26	210	35	46	25	97	161	61	36 (64)	16	30/13/6	2.7
MET-independent line														
SWB77	M-	ND	23	ND	4	19	10	8	274	165	410 (65)	29	94/25/87	0.3
Mut-p53	H48	ND		ND	4	19	11	6						
	H96	ND	61	ND	4	16	9	6	203	201	224 (88)	6	53/8/8	0.8
	H144	ND		ND	5	13	8	6						

NOTE. Densities were corrected for equal β-actin loading.
Abbreviations: MET, methionine; ND, not detectable; WT, wild-type.
* P-AKT 473 (308).
† P-Rb ser795/ser795/ser807/811.
‡ Ratio of Rb to P (ser807/811)-Rb.

methionine stress is indicative of the inhibitory effect of such stress on S entry in all of the methionine-dependent tumors and to some extent in SWB77. The most notable events in consequence to methionine stress in methionine-dependent tumors tested are the down-regulation of cyclin A1 and 2, cyclin B2, CDC2 and CDC25 (A and B), and BUB1, which is in agreement with the observed inhibition of mitosis. Down-regulation of CDC20 and that of CDC28 kinases is expected to contribute to the induction of mitotic checkpoints. Of particular interest is the marked reduction of P-Rb species, as compared with free Rb, which is expected to prevent entry into the S phase under methionine stress.

Transcription Factors. The transcriptional families that are affected during methionine stress are identified as follows: (*a*) AP-1, which regulates transcriptional control of c-JUN, JUN-B, c-FOS, and so forth; (*b*) c/EBP-β or γ; (*c*) the NF-κB subunits, p50 and p65; and (*d*) the early response gene BTG-1, c-MYC, and KROX-20. The c-JUN and JUN-B are up-regulated in DAOY and SWB61 by methionine stress and are also expressed in modest levels in all of the other tumors. A highly expressed in CNS tumors c/EBP-β (NF-IL6) is markedly up-regulated by methionine stress in all of the tumors, whereas c/EBP-γ is elevated in SWB61 and SWB40 but not in DAOY or SWB39. Activation of JNK pathway by methionine stress is in agreement with the overexpression of c-JUN (DAOY and SWB61) and c-MYC (SWB61 and 40), and it may be linked to the up-regulation of MKK4. The down-regulation of expression of ELK1 in SWB61 and 39 and of c-FOS in all of the methionine-dependent cell lines may be related to a modest down-regulation of PI3K by methionine stress. Transcriptional activation of NF-κB subunits p50 and p65 by methionine stress, in DAOY, SWB39, and SWB61 may be attributed to some extent in the persistent PI3K function and AKT
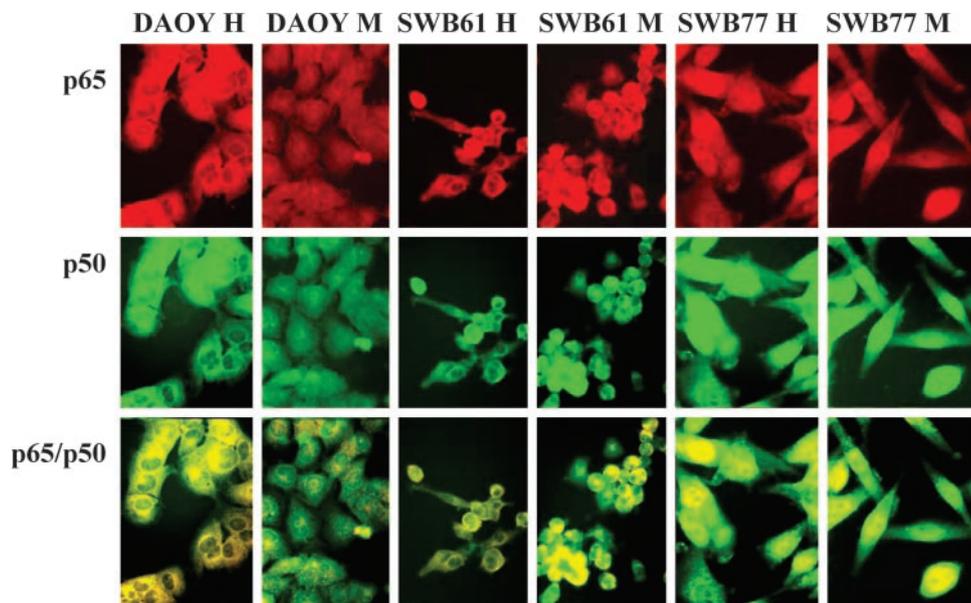

Fig. 5. Activation of NF-κB, as determined by colocalization (*yellow*) of NF-κB subunits p50 (*green*) and p65 (*red*) in the nucleus, was present in all of the cell lines tested and in SWB77 in particular. Methionine withdrawal results in the failure of NF-κB subunits to enter the nucleus in SWB61 and DAOY, but there were no substantial change in nuclear levels or colocalization of subunits in SWB77 under methionine stress. Methionine stress increases accumulation of NF-κB subunits in the cytosol.

7521

phosphorylation in these three lines but not in SWB40. Methionine stress enhances the expression of NF-κB subunits by a control that might also be related to interleukin production, but it fails to maintain its activation, which requires not only a functional PI3K but also the participation of H-Ras/MKK-3 activity, which is diminished under methionine stress (Fig. 6A). Failure to maintain active NF-κB is possibly linked to the suppression of E2F-1 response, which is reflected by the down-regulation of cyclins A/E and CDC2 in all of the methionine-dependent cell lines and by the diminished expression of polymerase α, dehydrofolate reductase, and thymidine kinase (11). Suppression of E2F-1 response is supported by the increase of Rb to P-Rb ratios, and it may be related to high levels of expression of p21 under methionine-stress conditions that prevent the dissociation of E2F-1 from Rb, despite declining levels of the latter. Up-regulation of p21 function is in accordance with the suppression of topoisomerase II, cyclin B, MMP1, MAP4, and MAD1 in the p53 competent lines SWB61 and 40 and to a lesser extent in DAOY and SWB39.

Cytokines and Related Pathways. Interleukins and their receptors are generally up-regulated in DAOY, SWB40, and SWB39 by methionine stress. Most remarkable is the induction of IL-8 in DAOY and SWB40. It is likely that IL-8 induces an AP-response in DAOY and SWB40 that is consistent with inhibition of NF-κB subunit transcription and subsequent activation (12–14). Methionine stress also results in up-regulation of the already highly expressed NF-IL6 and subsequent increase of the adrenomedullin signal (15) in all of the methionine-dependent cell lines. High expression of NF-IL6 and adrenomedullin is in agreement with the active involvement of phospholipase C and protein kinase C in SWB77, regardless of culture conditions. An impressive induction/up-regulation of the cytokines SCYA7, SCYA 20, and ST16 (MDA7 or IL24) is observed only in DAOY and in SWB39. SCYA20 induction correlates with up-regulation of TNF-α and related signal transduction pathways in these two lines (16). The induction of MDA7 in CNS tumors by methionine stress may be responsible for the several cytotoxic responses of methionine stress in DAOY. MDA7, also known as IL-24, is a novel cancer suppressing and apoptosis-inducing gene of the IL-10 family (17) with broad antitumor properties (18). In contrast to its antitumor effect, its expression, like methionine stress, does not induce toxicity in normal cells (17–23). MDA7 induces toxicity and apoptosis in many tumor cells containing various genetic defects such as p53, p16/INK4a, and/or Rb (17, 18, 22–24). The mechanism of action of the tumor suppressor MDA7 in melanoma involves up-regulation of the GADD family of genes including GADD 45-α, GADD 34, and GADD 153 and to a lesser extent GADD 45-γ with subsequent activation of p38 mitogen-activated protein kinase (MAPK) and the increase of the ratio of BAX to BCL-2 leading to apoptosis (21). Up-regulation of expression of c-JUN in DAOY by methionine stress and the absence of an effect in SWB77 are in agreement with patterns of MDA7 levels in these lines. Previous studies have shown induction of c-JUN by adenoviral delivery of MDA7 treatment of lung cancer cells (23). Up-regulation of IFN-γ and -β, TNF-α, IL-1B but not IL-12 or GM-CSF in DAOY, additionally support a functional MDA7 pathway under methionine stress. Furthermore, previous studies have shown that MDA7 treatment of human peripheral blood mononuclear cell results in induction of TH1 secondary cytokines, including IL-6, TNF-α, IFN-γ, and so forth (25). This study is the first linking endogenous MDA7 expression to growth control in CNS tumors, and correlates with previous studies in melanoma (17, 20). It is interesting that all of the methionine-dependent cell lines tested expressed low levels of MDA7 mRNA under normal growth conditions; however, when induced by methionine stress, both MDA7 mRNA and protein expression were rapidly and coordinately activated.

The inactivation of NF-κB by methionine stress despite the rise of IL-1 in DAOY is of interest. IL-1, like TNF-α, is a master inflammatory switch that initiates synthesis of a variety of factors including IL-6 and IL-8 (26), both of which alert the immune system. The action of IL-1 is mediated through binding to the interleukin Toll/IL-1 receptor superfamily, a member of receptors responding to injury and infection (27), and also by the activation of the IRAK-TRAF6 signaling module, which ultimately causes the release and nuclear translocation of NF-κB (26–29). The IL-1R–mediated signaling operates with the recruitment of Myd88 and Tollip, which activate IRAK-4, a kinase that phosphorylates and activates IRAK-1 (30). The module Myd88-IRAK–TRAF6 also controls signaling of p38 mitogen-activated protein kinase (MAPK), which, however, can be modulated by an IRAK-independent fashion involving Ras, TAB1-TAK1, and MKK3 with a direct effect on the activation of the transcription factors AFT2 and ELK1 (31). Activated TRAF and IRAK also interact with TGF-β–activated kinase TAK1 and with two TAK1 binding proteins, TAB1 and TAB2. Interaction of TAK1 and TAB1 with TRAF6 and IRAK induces TAK1 kinase, a mitogen activated protein kinase kinase kinase initially identified in the TGF signaling path. In turn, the activation of TAK1 results in phosphorylation of IKK and MAPK kinase (MKK3, 4, and 6) and inhibition of I-TRAF, leading to activation of NF-κB. An IRAK-independent pathway in NF-κB activation that uses TLR3, TRAF6, TAK1, TAB2, and PKR has been proposed, and it perhaps involve IKK, an inhibitor of I-TRAF (31, 32). I-TRAF is phosphorylated by inducible IKK-I and releases TRAF-2 from the I-TRAF.TRAF2 complex, which is then involved in activation of NF-κB (33). According to the above, the down-regulation of Myd88, IRAK-1, TAB1, and TAB2, when combined with the lack of IKK activation and the up-regulation of I-TRAF, are in agreement with inactivation of NF-κB under methionine stress in DAOY and other methionine-dependent CNS tumor cell lines.

TNF-α and Related Pathways. Methionine-stress results in a modest increase of TNF-α expression in DAOY. In the rest of the cells tested, TNF-α was expressed weakly. However, up-regulation of expression of TNF receptors in DAOY, SWB39, and especially SWB61 is likely to enhance TRAF2 degradation, an event that could determine the dominant cellular response phenotype of methionine stress via the TNF pathway (34, 35). That phenotype is proapoptotic, as contrasted with the proliferative NF-κB pathway supported by TRAF2. The most important event associated with TNF-α is the up-regulation of TRAIL in DAOY and SWB39 and that of TRAIL receptors in SWB61, 40, and 39 but not in SWB77. Therefore, the apoptotic response to methionine stress in methionine-dependent tumors is related to up-regulation of TRAIL (Fig. 6B), which in conjunction with DR6 and DR5 and the subsequent recruitment of FADD should result in caspase-8 activation (36). Of particular significance is that regulation of genes associated with the above pathways corroborates the observation that nuclear translocation of NF-κB subunits is abolished under methionine stress in DAOY despite marked up-regulation of expression of inflammatory cytokines. In addition, activation of NF-κB has been shown to inhibit the TNF-mediated apoptosis by triggering the expression of BCL-2 family of proteins and of the small death effectors domain containing the authentic protein NDED, also known as GG2–1 or SCC-S2 (37, 38). Sustained inhibition of NF-κB by I-kB suppresses the TNF-induced expression of NDED and IAP and facilitates the TNF-mediated activation of caspase 8 (37, 38). The TRAIL pathway is particularly favored in SWB61, in which high levels of expression of BAX (δ) and down-regulation of NDED and BCL-2 are in agreement with the activation of TNF receptor to suppress the NF-κB function.
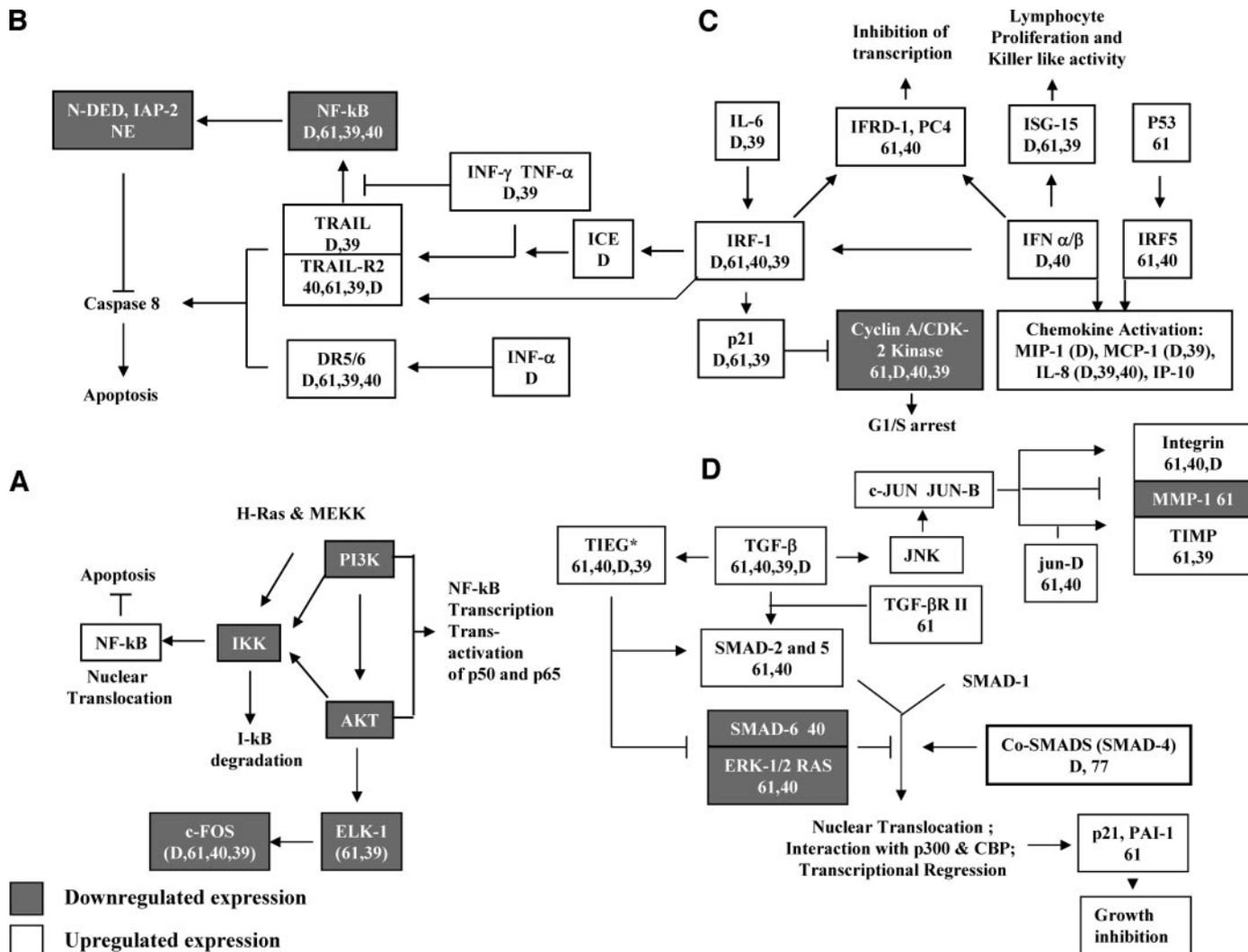
Fig. 6. *A.* Activation of NF-κB transcription requires only the PI3K/AKT pathway. Failure of methionine stress to activate the NF-κB in DAOY and SWB61, despite the observed up-regulation of p50 and p65-NF-κB, is attributed to the inhibition of both RAS and PI3K pathways by such stress. In DAOY, loss of NF-κB activation by methionine stress correlates with reduced AKT activation. In SWB61, 40 and 39 it correlates with apparent up-regulation of I-kB expression. *B.* TNF-α induces apoptosis via the up-regulation of TRAIL and TRAIL-R. TRAIL-induced apoptosis is enhanced by IFN-α through the up-regulation of the TRAIL death receptors DR-5 and 6. IFN-α represses TRAIL-activated NF-κB and augments the activation of caspase-8. IFN-γ induces FAS- and TNF-related apoptosis by inducing the ligand TRAIL and by up-regulating the expression of caspase-8 and -7. The opposite effect is expected in the absence of expression of death receptors in which case TRAIL activates NF-κB and the prosurvival NDED and IAP2. *C.* High levels of IRF-1 under methionine stress in DAOY result in the induction of ICE and TRAIL. Similarly, IRF-1 induces p53-independent up-regulation of p21 and/or inhibition of expression of cyclin A/CDC2 in DAOY, SWB61, 40 and 39. Transcriptional up-regulation of IFN-β in SWB39, 61 and particularly in SWB40 and DAOY is in agreement with high levels of expression of ISG-15 under methionine stress, which induces an inflammatory response. Up-regulation of MIP-1 (DAOY), MCP-1 (DAOY, SWB39), and IL-8 (DAOY, SWB39, and SWB40) is in accordance with the increase of IFN signal primarily in DAOY and also in SWB39, 40 and 61. *D.* Proteins of the TGF-β superfamily activate intracellular signals by phosphorylating SMAD proteins. Activated R-SMADs form complexes with Co-SMADs and translocate into the nucleus where they regulate transcription of target genes. ISMADs function as antagonists of TGF-β/BMP signaling by interacting with type I receptors and competing with R-SMADs. NonSMAD pathways activated by TGF-β include ERK/MAPK, JNK, AKT, and p53 MAP kinases. TGF-β induces growth inhibition, which is mediated by repression of c-MYC, induction of p21, and p15 CDK inhibitors, and CDC25A. This pathway appears to be activated in SWB61 and 40 and to some extent in SWB39 and DAOY. In SWB61 and 40 it is possibly mediated via induction of TIEG, up-regulation of SMAD-2, and down-regulation of SMAD-6. Documented marked up-regulation of TGF-β signal in SWB61 is accompanied by enhanced expression of TIEG, apparent activation of SMAD-2, and down-regulation of SMAD-6 and 7 expression. The combined effect as expected is the activation of JNK as determined by the up-regulation of expression of JUN-D, B, and c-JUN, as well as the marked up-regulation of TIMP and integrin. Furthermore, the effect of TGF-β on proapoptotic and cell cycle inhibition in SWB61 by methionine-stress is documented by the increased expression of PAI-1 and p21 and the induction of ERK2. On the other hand, the expected up-regulation of AKT at ser 473 as a result of TGF-β up-regulation is maintained under methionine stress in SWB61, whereas such phosphorylation is reduced in DAOY, 40 and even in SWB77.

Effect of Methionine Stress on Interferon-regulated Pathways. Up-regulation of IRF-1 by methionine stress is expected to promote apoptosis by regulating the expression of caspases, Fas/CD95, Fas ligand, and BCL-2 (39–45). The robust inductive effect of methionine stress on TRAIL and DR6, and a correlation between IRF-1, TRAIL and DR6 up-regulation under methionine stress in DAOY, suggests that IRF-1 may precede the induction of TRAIL (Fig. 6*C*) and that a pathway involving both IRF-1 and TRAIL could be a major route leading to apoptosis (46, 47). This response is not fully operational in SWB61 in which up-regulation of IRF-1 does not enhance expression of IFN-β and appears to proceed exclusively via the IFN-γ–mediated pathway. The antiprolifera-

tive and proapoptotic activity of IRF-1 is also mediated via the activation of p21, which induces growth arrest in G_0/G_1 by inhibiting cyclin A/CDK2 kinase (48, 49). Interferon-mediated growth arrest via the induction of p21 is most likely to occur in DAOY, in which p21 protein levels rise by at least 20-fold. Induction of PC4 in SWB61 and SWB40 by IRF-1 or IFN-α/β additionally limits promoter-driven transcription as well as nonspecific transcription, which is additionally enhanced by the nonexpression of TFIIH and the suppression of ERCC3 expression (50). Another pathway involving IRF-1 in DAOY could be mediated by the induction of IFN α and β, which up-regulate synthesis of ISG15 and suppress proliferation (49, 50).

TGF-β–Regulated Pathways. TGF-β is a potent growth inhibitor exerting its effect by binding to specific type I and II receptors, which in turn initiate intracellular signaling via the SMAD proteins. Phosphorylated SMADS translocate to the nucleus and modulate target gene transcription resulting in down-regulation of c-JUN, c-FOS, c-MYC, CDC25, up-regulation of p21, p15, and the plasminogen activator inhibitors 1 and 2 (51–56). In addition, TGF-β initiates signal transduction pathways, including AKT (AKT phosphorylation at Ser-473), stress-activated protein kinase/JUN-N terminal kinase (SAPK/JNK), AP-1, p38/MAPK, ERK 1 and 2, and MAPK (57–58). TGF-β signal is up-regulated by methionine stress predominantly in SWB61 and 40 (Fig. 6D), indicating that regulation of growth in these lines under methionine stress is controlled by the TGF-β pathway. The R-SMADs, SMAD 2 and 5 are induced in SWB61 and 40, whereas the I-SMADS, SMAD 6 and 7 are transcriptionally down-regulated or unaffected under methionine stress in DAOY and SWB40 in particular. This pattern of SMAD activation could be a response to the up-regulation of the TGF-β–inducible early gene (TIEG), a transcriptional regulator of thyroid hormone receptor as well as of the TGF-β receptor itself (51, 59–61). TIEG amplifies the effect of R-SMADS, triggers expression of p21, enhances TGF-mediated expression of SMAD2, and represses expression of SMAD6 (61–64). In addition, SMAD-dependent mechanisms are responsible for the activation of both the c-JUN and JUN-B promoters by TGF-β (63), which could also apply in the case of the response of glial tumors to methionine-stress. TGF-β has been shown to repress MMP1 by altering ratios of B-JUN, JUN-D, or c-JUN containing AP-1 complexes. The modulation of expression of these gene products under methionine stress is in accordance with the control of TIMP1 and MMP1 expression via the TGF-β pathway in SWB61 and SWB40 (63).

The Effect of p53 Mutational Status on Methionine Stress. Given the many potential binding sites for p53 (>100), it is likely that tumor growth suppression by p53 is achieved by regulating the physiologic function of a multitude of genes (65). IRF-5 has been shown to be a direct target for p53, and as such, it may respond to stress that affects p53 expression (66). Methionine stress up-regulates p53-regulated genes GADD45, BRCA-1, and p21 in mut p53 DAOY and SWB39. This indicates that these genes are not always dependent on wt-p53 function and can be induced regardless of the mutational status of p53. The only exception is the resistant line SWB77, which did not respond to methionine stress and expressed the same or lower levels of GADDs under methionine stress. The ability of methionine stress to induce p21 and GADDs independently of wt-p53 is expected to steer p53-mutant cells toward death by acting in lieu of wt p53, thus causing a switch from a proliferative state to an apoptotic one. Nevertheless, the role of wt-p53 in enhancing the effect of methionine stress is evident, considering differences in the resistance between SWB61, in which p53 is up-regulated, and SWB40, in which methionine stress has no effect on its expression.

In summary, methionine stress results in partial suppression of PI3K/AKT and RAF/RAS proliferative/prosurvival pathways and inactivation of NF-κB in all of the methionine-dependent tumors. MDA7 protein levels increase by >60- to 100-fold in DAOY and SWB39, and p21 is up-regulated in these cells in a p53-independent manner. MDA7 induction and TNF-α activation of TRAIL, its receptor, and of DR6 are most likely responsible for apoptotic events in SWB39 and DAOY. Of particular interest is the marked induction of the cytokines IL-1, IL-8, IL-6, SCYA20, SCYA7, and IL-24 primarily in DAOY and to some extent in SWB39 by methionine stress. The up-regulation of IL-6 in DAOY and SWB61 by methionine stress could be associated to induction of IRF-1 and subsequently to up-regulation of p21 as well as to the activation of TRAIL and the TRAIL receptor 3. These events could lead to a p53-independent cell cycle arrest and death. The induction of PC4 and IFRD-1 in SWB61 and 40 could be linked to inhibition of transcription, whereas induction of ISG15 by IFN-β could lead to an inflammatory response under methionine stress. Activation of the IFN regulated pathways is fully supported by the induction of MIP1, MCP1, IL-8, and IP-10 genes in DAOY and to a lesser extent in SWB39 and 40. The wt-p53 in SWB61 may contribute directly to cell death via the induction of BAX and down-regulation of BCL-2. Whereas the MDA7, TNF, and IFN-regulated pathways are likely to be involved in induction of proapoptotic and antiproliferative responses in DAOY, the TGF-β pathway appears to be primarily involved in the toxicity of methionine stress in SWB61. The postulated mechanism for the TGF-β-mediated effect on SWB61 and to a lesser extent on SWB40, SWB39, and DAOY is mediated via the induction of the R-SMADS 2 and 5 and the down-regulation of I-SMAD 6. This mechanism is also supported by the up-regulation of expression of TIEG and by the marked induction of TIMP in SWB61. Cell cycle control in response to TGF-β is induced by the up-regulation of ERK2 and induction of p21 and PAI1.

REFERENCES

1. Halpern BC, Clark BR, Hardy DN, Halpern RM, Smith RA. The effect of replacement of MET by homocystine on survival of malignant and normal adult mammalian cells in culture. Proc Natl Acad Sci USA 1974;71:1133–6.
2. Judde JG, Ellis M, Frost P. Biochemical analysis of the role of transmethylation in the MET dependence of tumor cells. Cancer Res 1989;49:4859–65.
3. Kokkinakis DM, Hoffman RM, Frenkel EP, et al. Synergy between MET stress and chemotherapy in the treatment of brain tumor xenografts in athymic mice. Cancer Res 2001;61:4017–23.
4. Kokkinakis DM, Wick JB, Zhou QX. Metabolic response of normal and malignant tissue to acute and chronic MET stress in athymic mice bearing human glial tumor xenografts. Chem Res Toxicol 2002;15:1472–9.
5. Kokkinakis DM, Schold SC Jr, Hori H, Nobori T. Effect of long-term depletion of plasma MET on the growth and survival of human brain tumor xenografts in athymic mice. Nutr Cancer 1997;29:195–204.
6. Kokkinakis DM, von Wronski MA, Vuong TH, Brent TP, Schold SC Jr. Regulation of O6- methylguanine-DNA methyltransferase by MET in human tumour cells. Br J Cancer 1997;75:779–88.
7. Bocangel DB, Finkelstein S, Schold SC, et al. Multifaceted resistance of gliomas to temozolomide. Clin Cancer Res 2002;8:2725–34.
8. Lupberger J, Kreuzer KA, Baskaynak G, et al. Quantitative analysis of beta-actin, beta-2-microglobulin and porphobilinogen deaminase mRNA and their comparison as control transcripts for RT-PCR. Mol Cell Probes 2002;16:25–30.
9. Rao PN, Johnson RT. Mammalian cell fusion: studies on the regulation of DNA synthesis and mitosis. Nature (Lond) 1970;225:159–64.
10. Nurse P. A long twentieth century of the cell cycle and beyond. Cell 2000;100:71–8.
11. Verona R, Moberg K, Estes S, et al. E2F activity is regulated by cell cycle-dependent changes in subcellular localization. Mol Cell Biol 1997;17:7268–82.
12. Mukaida N, Mahe Y, Matsushima K. Cooperative interaction of nuclear factor-kappa B- and cis-regulatory enhancer binding protein-like factor binding elements in activating the interleukin-8 gene by pro-inflammatory cytokines. J Biol Chem 1990;265:21128–33.
13. Yasumoto K, Okamoto S, Mukaida N, et al. Tumor necrosis factor alpha and interferon gamma synergistically induce interleukin 8 production in a human gastric cancer cell line through acting concurrently on AP-1 and NF-kB-like binding sites of the interleukin 8 gene. J Biol Chem 1992;267:22506–11.
14. Brasier AR, Jamaluddin M, Casola A, et al. A promoter recruitment mechanism for tumor necrosis factor-alpha-induced interleukin 8 transcription in type II pulmonary epithelial cells. Dependence on nuclear abundance of Rel A, NF-kappaB1, and c-Rel transcription factors. J Biol Chem 1998;273:3551–61.
15. Ishimitsu T, Tsukada K, Minami J, Ono H, Matsuoka H. Variations of human adrenomedullin gene and its relation to cardiovascular diseases. Hypertens Res 2003;26(Suppl):S129–34.
16. Harant H, Eldershaw SA, Lindley IJ. Human macrophage inflammatory protein-3alpha/CCL20/LARC/Exodus/SCYA20 is transcriptionally upregulated by tumor necrosis factor-alpha via a nonstandard NF-kappaB site. FEBS Lett 2001;509:439–45.
17. Chada S, Sutton RB, Ekmekcioglu S, et al. MDA7/IL-24 is a unique cytokine in the IL-10 family. Int Immunopharmacol 2004;4:649–67.
18. Jiang H, Su ZZ, Lin JJ, et al. The melanoma differentiation associated gene MDA7 suppresses cancer cell growth. Proc Natl Acad Sci USA 1996;93:9160–5.
19. Su ZZ, Madireddi MT, Lin JJ, et al. The cancer growth suppressor gene MDA7 selectively induces apoptosis in human breast cancer cells and inhibits tumor growth in nude mice. Proc Natl Acad Sci USA 1998;95:14400–5.
20. Ekmekcioglu S, Ellerhorst J, Mhashilkar A, et al. Down-regulation of melanoma differentiation associated gene (MDA7) expression in human melanomas. Int J Cancer 2001;94:54–9.
21. Sarkar D, Su ZZ, Lebedeva IV, et al. MDA7 (IL-24) mediates selective apoptosis in human melanoma cells by inducing the coordinated overexpression of the GADD family of genes by means of p38 MAPK. Proc Natl Acad Sci USA 2002;99:10054–9.

22. Mhashilkar AM, Schrock RD, Hindi M, et al. Melanoma differentiation associated gene-7 (MDA7): a novel anti-tumor gene for cancer gene therapy. Mol Med 2001; 7:271–82.

23. Kawabe S, Nishikawa T, Munshi A, et al. Adenovirus mediated MDA7 gene expression radiosensitizes non-small lung cancer cells via p53-independent mechanisms. Mol Ther 2002;6:637–44.

24. Rampino N, Yamamoto H, Ionov Y, et al. Somatic frameshift mutations in the BAX gene in colon cancers of the microsatellite mutator phenotype. Science (Wash DC) 1997;275:967–9.

25. Caudell EG, Mumm JB, Poindexter N, et al. The protein product of the tumor suppressor gene, melanoma differentiation-associated gene 7, exhibits immunostimulatory activity and is designated IL-24. J Immunol 2002;168:6041–6.

26. Neumann D, Lienenklaus S, Rosati O, Martin MU. IL-1beta-induced phosphorylation of PKB/Akt depends on the presence of IRAK-1. Eur J Immunol 2002;32:3689–98.

27. Bowie A, O'Neill LA. The interleukin-1 receptor/Toll-like receptor superfamily: signal generators for pro-inflammatory interleukins and microbial products. J Leukoc Biol 2000;67:508–14.

28. Rock FL, Hardiman G, Timans JC, Kastelein RA, Bazan JF. A family of human receptors structurally related to Drosophila Toll. Proc Natl Acad Sci USA 1998;95: 588–93.

29. Janssens S, Beyaert R. Functional diversity and regulation of different interleukin-1 receptor-associated kinase (IRAK) family members. Mol Cell 2003;11:293–302.

30. Janssens S, Burns K, Tschopp J, Beyaert R. Regulation of interleukin-1- and lipopolysaccharide-induced NF-kappaB activation by alternative splicing of MyD88. Curr Biol 2002;12:467–71.

31. Jiang Z, Zamanian-Daryoush M, Nie H, et al. Poly(I-C)-induced Toll-like receptor 3 (TLR3)-mediated activation of NFkappa B and MAP kinase is through an interleukin-1 receptor-associated kinase (IRAK)-independent pathway employing the signaling components TLR3-TRAF6-TAK1-TAB2-PKR. J Biol Chem 2003;278: 16713–19.

32. Nomura F, Kawai T, Nakanishi K, Akira S. NF-kappaB activation through IKK-i-dependent I-TRAF/TANK phosphorylation. Genes Cells 2000;5:191–202.

33. Baltathakis I, Alcantara O, Boldt DH. Expression of different NF-kappaB pathway genes in dendritic cells (DCs) or macrophages assessed by gene expression profiling. J Cell Biochem 2001;83:281–90.

34. Wajant H, Henkler F, Scheurich P. The TNF-receptor-associated factor family: scaffold molecules for cytokine receptors, kinases and their regulators. Cell Signal 2001;13:389–400.

35. Acharya A, Singh SM. Effect of TNF-alpha on the induction of apoptosis in murine macrophages: role of interleukin-1 beta converting enzyme. Int J Immunopathol Pharmacol 2001;14:5–10.

36. Rossi D, Gaidano G. Messengers of cell death: apoptotic signaling in health and disease. Haematologica 2003;88:212–8.

37. You Z, Ouyang H, Lopatin D, Polver PJ, Wang CY. Nuclear factor-kappa B-inducible death effector domain-containing protein suppresses tumor necrosis factor-mediated apoptosis by inhibiting caspase-8 activity. J Biol Chem 2001;276:26398–404.

38. Kumar D, Whiteside TL, Kasid U. Identification of a novel tumor necrosis factor-alpha-inducible gene, SCCS2, containing the consensus sequence of a death effector domain of fas-associated death domain-like interleukin-1beta-converting enzyme-inhibitory protein. J Biol Chem 2000;275:2973–8.

39. Taniguchi T, Takaoka A. A weak signal for strong responses: interferon-alpha/beta revisited. Nat Rev Mol Cell Biol 2001;2:378–86.

40. Kim KB, Choi YH, Kim IK, et al. Potentiation of Fas- and TRAIL-mediated apoptosis by IFN-gamma in A549 lung epithelial cells: enhancement of caspase-8 expression through IFN-response element. Cytokine 2002;20:283–8.

41. Kumar A, Commane M, Flickinger TW, Horvath CM, Stark GR. Defective TNF-alpha-induced apoptosis in STAT1-null cells due to low constitutive levels of caspases. Science (Wash DC) 1997;278:1630–2.

42. Sedger LM, Shows DM, Blanton RA, et al. IFN-gamma mediates a novel antiviral activity through dynamic modulation of TRAIL and TRAIL receptor expression. J Immunol 1999;163:920–6.

43. Park SY, Billiar TR, Seol DW. IFN-gamma inhibition of TRAIL-induced IAP-2 upregulation, a possible mechanism of IFN-gamma-enhanced TRAIL-induced apoptosis. Biochem Biophys Res Commun 2002;291:233–6.

44. Tomita Y, Bilim V, Hara N, Kasahara T, Takahashi K. Role of IRF-1 and caspase-7 in IFN-gamma enhancement of Fas-mediated apoptosis in ACHN renal cell carcinoma cells. Int J Cancer 2003;104:400–8.

45. Shigeno M, Nakao K, Ichikawa T, et al. Interferon-alpha sensitizes human hepatoma cells to TRAIL-induced apoptosis through DR5 upregulation and NF-kappa B inactivation. Oncogene 2003;22:1653–62.

46. Kirchhoff S, Schaper F, Hauser H. Interferon regulatory factor 1 (IRF-1) mediates cell growth inhibition by transactivation of downstream target genes. Nucleic Acids Res 1993;21:2881–9.

47. Wessely R, Hengst L, Jaschke B, et al. A central role of interferon regulatory factor-1 for the limitation of neointimal hyperplasia. Hum Mol Genet 2003;12:177–87.

48. Yonemitsu Y, Kaneda Y, Tanaka S, et al. Transfer of wild-type p53 gene effectively inhibits vascular smooth muscle cell proliferation in vitro and in vivo. Circ Res 1998;82:147–56.

49. D'Cunha J, Knight E Jr, Haas AL, Truitt RL, Borden EC. Immunoregulatory properties of ISG15, an interferon-induced cytokine. Proc Natl Acad Sci USA 1996;93: 211–5.

50. Fukuda A, Tokonabe S, Hamada M, et al. Alleviation of PC4- mediated transcriptional repression by the ERCC3 helicase activity of general transcription factor TFIIH. J Biol Chem 2003;278:14827–31.

51. Johnsen SA, Subramaniam M, Katagiri T, Janknecht R, Spelsberg TC. Transcriptional regulation of Smad2 is required for enhancement of TGFbeta/Smad signaling by TGFbeta inducible early gene. J Cell Biochem 2002;87:233–41.

52. Goumans MJ, Mummery C. Functional analysis of the TGFbeta receptor/Smad pathway through gene ablation in mice. Int J Dev Biol 2000;44:253–65.

53. Miyazono K, Suzuki H, Imamura T. Regulation of TGF-beta signaling and its roles in progression of tumors. Cancer Sci 2003;94:230–4.

54. ten Dijke P, Miyazono K, Heldin CH. Signaling inputs converge on nuclear effectors in TGF-beta signaling. Trends Biochem Sci 2000;25:64–70.

55. Johnsen SA, Subramaniam M, Janknecht R, Spelsberg TC. TGFbeta inducible early gene enhances TGFbeta/Smad-dependent transcriptional responses. Oncogene 2002; 21:5783–90.

56. Bakin AV, Tomlinson AK, Bhowmick NA, Moses HL, Arteaga CL. Phosphatidylinositol 3-kinase function is required for transforming growth factor beta-mediated epithelial to mesenchymal transition and cell migration. J Biol Chem 2000;275: 36803–10.

57. Hocevar BA, Brown TL, Howe PH. TGF-beta induces fibronectin synthesis through a c-Jun N-terminal kinase-dependent, Smad4-independent pathway. EMBO J 1999; 18:1345–56.

58. Imai K, Takeshita A, Hanazawa S. TGF-beta inhibits lipopolysaccharide-stimulated activity of c-Jun N-terminal kinase in mouse macrophages. FEBS Lett 1999;456: 375–8.

59. Sano Y, Harada J, Tashiro S, et al. ATF-2 is a common nuclear target of Smad and TAK1 pathways in transforming growth factor-beta signaling. J Biol Chem 1999; 274:8949–57.

60. Dennler S, Itoh S, Vivien D, et al. Direct binding of Smad3 and Smad4 to critical TGF beta-inducible elements in the promoter of human plasminogen activator inhibitor-type 1 gene. EMBO J 1998;17:3091–100.

61. Moustakas A, Kardassis D. Regulation of the human p21/WAF1/Cip1 promoter in hepatic cells by functional interactions between Sp1 and Smad family members. Proc Natl Acad Sci USA 1998;95:6733–8.

62. Verrecchia F, Tacheau C, Schorpp-Kistner M, Angel P, Mauviel A. Induction of the AP-1 members c-Jun and JunB by TGF-beta/Smad suppresses early Smad-driven gene activation. Oncogene 2001;20:2205–11.

63. Hall MC, Young DA, Waters JG, et al. The comparative role of activator protein 1 and Smad factors in the regulation of Timp-1 and MMP-1 gene expression by transforming growth factor-beta 1. J Biol Chem 2003;278:10304–13.

64. Frey RS, Mulder KM. Involvement of extracellular signal-regulated kinase 2 and stress-activated protein kinase/Jun N-terminal kinase activation by transforming growth factor beta in the negative growth control of breast cancer cells. Cancer Res 1997;57:628–33.

65. Hirao A, Kong YY, Matsuoka S, et al. DNA damage-induced activation of p53 by the checkpoint kinase Chk2. Science (Wash DC) 2000;287:1824–7.

66. Mori T, Anazawa Y, Iiizumi M, et al. Identification of the interferon regulatory factor 5 gene (IRF-5) as a direct target for p53. Oncogene 2002;21:2914–18.

Modulation of Gene Expression in Human Central Nervous System Tumors under Methionine Deprivation-induced Stress

Demetrius M. Kokkinakis, Xiaoyan Liu, Sunil Chada, et al.

Updated version	Access the most recent version of this article at: http://cancerres.aacrjournals.org/content/64/20/7513
Supplementary Material	Access the most recent supplemental material at: http://cancerres.aacrjournals.org/content/suppl/2005/06/08/64.20.7513.DC1

Cited articles	This article cites 65 articles, 32 of which you can access for free at: http://cancerres.aacrjournals.org/content/64/20/7513.full#ref-list-1
Citing articles	This article has been cited by 5 HighWire-hosted articles. Access the articles at: http://cancerres.aacrjournals.org/content/64/20/7513.full#related-urls

E-mail alerts	Sign up to receive free email-alerts related to this article or journal.
Reprints and Subscriptions	To order reprints of this article or to subscribe to the journal, contact the AACR Publications Department at pubs@aacr.org.
Permissions	To request permission to re-use all or part of this article, use this link http://cancerres.aacrjournals.org/content/64/20/7513. Click on "Request Permissions" which will take you to the Copyright Clearance Center's (CCC) Rightslink site.